

Hidden Higgs Decaying to Lepton Jets

Adam Falkowski^a, Joshua T. Ruderman^b, Tomer Volansky^c and Jure Zupan^d

^a *NHETC and Department of Physics and Astronomy,
Rutgers University, Piscataway, NJ 08854, USA*

^b *Department of Physics, Princeton University, Princeton, NJ 08544*

^c *School of Natural Sciences, Institute for Advanced Study, Princeton, NJ 08540*

^d *Faculty of Mathematics and Physics, University of Ljubljana
Jadranska 19, 1000 Ljubljana, Slovenia*

Abstract

The Higgs and some of the Standard Model superpartners may have been copiously produced at LEP and the Tevatron without being detected. We study a novel scenario of this type in which the Higgs decays predominantly into a light hidden sector either directly or through light SUSY states. Subsequent cascades increase the multiplicity of hidden sector particles which, after decaying back into the Standard Model, appear in the detector as clusters of collimated leptons known as lepton jets. We identify the relevant collider observables that characterize this scenario, and study a wide range of LEP and Tevatron searches to recover the viable regions in the space of observables. We find that the Higgs decaying to lepton jets can be hidden when the event topology mimics that of hadronic backgrounds. Thus, as many as 10^4 leptonic Higgs and SUSY decays may be hiding in the LEP and Tevatron data. We present benchmark models with a 100 GeV Higgs that are consistent with all available collider constraints. We end with a short discussion of strategies for dedicated searches at LEP, the Tevatron and the LHC, that allow for a discovery of the Higgs or SUSY particles decaying to lepton jets.

Contents

1	Introduction	2
2	The Hidden Sector	6
2.1	Portals	6
2.2	A Minimal Model	8
3	Higgs Decays to the Hidden Sector	9
3.1	Neutralino Channel	10
3.2	Sneutrino Channel	13
3.3	Singlet Channel	14
4	Collider Phenomenology	15
4.1	Lepton Jets and Neutralino Jets	16
4.2	Experimental Observables	17
5	Can Lepton Jets Really Hide the Higgs?	23
6	Experimental Constraints	23
6.1	LEP-1 Searches	24
6.2	LEP-2 Searches	26
6.3	Tevatron Searches	28
7	Hiding the Higgs	29
7.1	Methodology	29
7.2	Constraints on Experimental Observables	30
7.3	Benchmarks Models	33
8	Suggested Search Strategies	37
9	Conclusions and Outlook	39
A	Notation	41

1 Introduction

Within the Standard Model (SM) the mass of the Higgs boson is constrained by the LEP experiments to be larger than 114.4 GeV [1]. This limit, however, varies in a model-dependent manner. For example, the limit can be relaxed if the production cross-section of the Higgs particle is suppressed. A more interesting possibility is that the *Higgs is hidden: it has been copiously produced at LEP and the Tevatron but has evaded detection due to non-standard decays*. There are at least two hints that the Higgs might be lighter than the naive LEP limit. On the experimental side, the best fit to electroweak precision observables corresponds to a Higgs mass of 80 GeV [2]. On the theoretical side, typical supersymmetric models require fine-tuning to accommodate a Higgs boson substantially heavier than m_Z .

The naive LEP limit on the Higgs mass is based on studies of the associated production of the Higgs and Z -boson, with the Higgs decaying to a pair of b quarks (as in the SM). In theories beyond the SM, the Higgs decay pattern can be greatly modified [3]. Then, as long as the $h \rightarrow b\bar{b}$ branching ratio is below $\lesssim 20\%$, the standard Higgs search strategies and mass limits may not directly apply [4]. The LEP collaborations have put considerable effort into constraining non-standard Higgs decays into invisible particles or into final states with two SM particles. However, Higgs decays into higher multiplicity final states have not been systematically searched for. Consequently, it is conceivable that the Higgs decaying in a non-standard way may have been missed at colliders, if it decays into a final state that has not been targeted. In reality, it is not necessarily easy for a light Higgs to remain hidden, because the collective body of LEP searches constrain many different final state topologies. Even if a specific Higgs decay mode has not been searched for directly, it may still be captured by a multitude of LEP searches.

There are a few proposals for a hidden Higgs in the literature (for a review see [5, 6]). The most studied scenario (and the first one to point out the improved naturalness with a hidden Higgs) is in the context of the NMSSM [7]. Additional examples include more general singlet extensions of the MSSM [8], supersymmetric little Higgs models [9], the R-parity violating MSSM [10], and the CP-violating MSSM [11]. In all of these scenarios the Higgs decays into

a pair of light non-SM particles, e.g. pseudoscalar singlets or neutralinos, which then decay into two or more visible SM particles. Recently, the hidden Higgs scenario has triggered enough interest in the community to prompt the revisiting of LEP data in search of certain 4-body Higgs decay topologies. The $h \rightarrow 4b$ [4] and $h \rightarrow 4\tau$ [12] possibilities are now excluded for Higgs masses $\lesssim 110$ GeV. Other scenarios, however, are constrained only by the model-independent Higgs search of OPAL [13], requiring that the Higgs mass be above ~ 82 GeV.

The hidden Higgs idea is most naturally expressed in the context of supersymmetry (SUSY) where the existence of a light Higgs, $m_h \simeq m_Z$, ameliorates the little hierarchy problem. In this case it is natural to wonder whether *SUSY could also be hidden*: some of the SM superpartners may have been copiously produced at colliders and evaded detection due to non-standard decays. In this paper, we realize hidden Higgs and hidden SUSY in a supersymmetric model with a light hidden sector. The lightest ‘visible’ superpartner (LVSP – the equivalent of the LSP in the MSSM) is allowed to cascade into the hidden sector, typically producing visible particles in the process. The sensitivity of standard SUSY searches can then be greatly diminished when the LVSP decays partly into visible energy.

We consider three distinct scenarios where the lightest MSSM Higgs boson decays dominantly into the hidden sector. In the *singlet channel* scenario the Higgs decays to the hidden sector through direct couplings. In the other two scenarios the Higgs first decays to a pair of LVSPs which, having no visible decay channels open, decay into the hidden sector. The MSSM contains two types of electrically neutral and colorless superpartners which leads to the *neutralino channel* and the *sneutrino channel* scenarios. In all of the models we consider, hidden sector cascades produce a large multiplicity of boosted hidden sector particles. Some of these hidden sector particles decay to leptons, and the final state of the Higgs decay is therefore characterized by several groups of collimated leptons plus missing energy. The name *lepton jet* has been coined for these spectacular objects [14, 15, 16].

The striking phenomenology of light hidden sectors has been studied in the past [17]. More recently, the existence of such sectors was motivated by the observed astrophysical anomalies [18, 19, 20]. Indeed, the observed excesses in the positron and electron cosmic ray fluxes may be signatures of dark matter annihilations [21, 22, 23, 24, 25, 26] or decays [22, 27] into a light hidden sector which is weakly coupled to the visible sector. In this paper we do

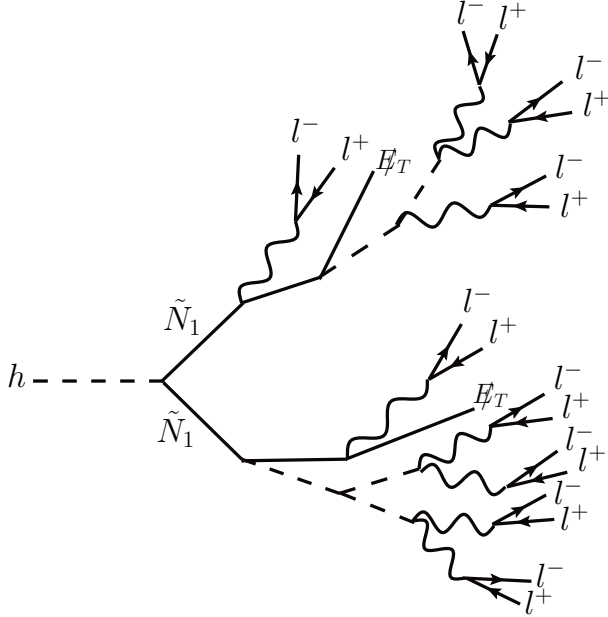


Figure 1: An example of a Higgs decay to lepton jets, through the neutralino production portal of Section 3.1. The hidden sector cascades can lead to many leptons per Higgs decay, in this case 18. This example uses the particle content and vertices of the minimal $U(1)_d$ hidden sector described in section 2.2. A larger hidden sector can lead to even larger multiplicities. If the neutralinos are heavy enough to be produced close to rest, their decay products will be well-separated, and the leptons will partition into 4 distinct lepton jets. Alternatively, if the neutralinos are light and boosted, the event will consist of two groups of collimated leptons, *neutralino jets*.

not address the aforementioned anomalies and concentrate instead, on the collider signatures of such hidden sectors.

As a simple example, we consider a hidden sector with $U(1)_d$ gauge symmetry broken at the GeV scale. $U(1)_d$ couples to the visible sector through kinetic mixing with hypercharge, implying that (i) the hidden photon can decay to the light SM fermions, and (ii) the LVSP can decay to the hidden sector. Consequently, once the Higgs decays, it initiates a hidden sector cascade, producing in addition to the true LSP, many hidden photons and scalars which decay to highly boosted lepton jets. An example of such a Higgs decay is shown in Fig. 1. To demonstrate that a light Higgs can be accommodated in the above scenario, we simulate Higgs decays to lepton jets and determine the sensitivity of a wide range of LEP and Tevatron searches. We consider the experimental observables that are relevant for Higgs

decays into lepton jets, and identify the viable region in the space of these observables. This procedure allows us to write benchmark models for the neutralino and singlet channels in which the Higgs as light as 100 GeV is allowed by all existing searches. (The sneutrino channel is harder to accommodate with the specific hidden sector we consider.) One should stress that the final states in these models are so spectacular that a *dedicated* analysis at LEP or the Tevatron could quickly discover the Higgs signal, or place a far more stringent bound on the Higgs boson mass.

Several previous studies have considered Higgs decays to light hidden sectors. Ref. [28] considers decays that produce very displaced vertices. While it is conceivable that such a scenario can accommodate a light Higgs, this possibility was not explored by the authors of [28] and we do not consider it here. Ref. [29] discusses Higgs decays to two hidden sector photons which subsequently decay to four SM leptons [29]. The authors do not attempt to hide a light Higgs in this scenario (but see comments in [6]). We take a complimentary approach by considering different models that yield a larger variety of final state topologies and multiplicities than these previous works, and in doing so, we identify scenarios that allow for a light Higgs boson with prompt decays.

This paper is organized as follows. In Section 2 we review the concept of a GeV-scale hidden sector that communicates with the SM through kinetic mixing, and introduce a minimal phenomenological model with a $U(1)_d$ gauge symmetry. In Section 3 we describe the channels via which the Higgs can decay into the hidden sector. In Section 4 we discuss the collider phenomenology of Higgs decays to lepton jets by defining the experimental observables that characterize this scenario. In Section 5 we briefly explain why a light Higgs decaying into lepton jets is not obviously excluded by LEP and Tevatron searches, as one may naively suspect. We then review the relevant LEP and Tevatron searches in Section 6. In Section 7, we discuss how these searches constrain the experimental observables, and construct benchmark models with a 100 GeV Higgs that satisfy these constraints. In Section 8 we discuss search strategies at LEP and the Tevatron that can differentiate lepton jets from QCD jets and allow for discovery of a light Higgs decaying to lepton jets. We conclude in Section 9. We describe our hidden sector notations in Appendix A and list benchmark signal efficiencies for LEP and Tevatron searches in Appendix B.

2 The Hidden Sector

We begin by reviewing the framework in which we will later embed a hidden Higgs. In Section 2.1, we discuss portals that can connect a light hidden sector to the visible sector. These portals take the form of operators composed of both hidden sector fields and SM fields. We focus on the vector portal – kinetic mixing between hidden sector gauge fields and SM gauge fields. Then, in Section 2.2, we specialize to a minimal phenomenological hidden sector, with $U(1)_d$ gauge symmetry, and discuss the interactions among hidden sector fields. These hidden sector interactions will be important for the collider phenomenology discussed later in the paper.

2.1 Portals

To trigger non-conventional Higgs decays, we study a hidden sector with a gauge group G_d broken at the GeV scale and weakly coupled to the SM. Here and below we work in the supersymmetric framework, which allows one to stabilize both the weak and GeV scales. For simplicity, we will focus on $G_d = U(1)_d$. We will see that this simple case is rich enough to allow for Higgs decays with tens of lepton tracks. Non-Abelian models generalize the structure and provide a simple way to further soften and increase the multiplicity of the produced leptons. We return to this scenario in Section 7.3.

The hidden sector may couple to the visible sector through various portals (for a useful discussion see [30]). Here we concentrate on the so-called *vector portal* which has been studied extensively [31, 32, 30, 21, 16, 33, 34, 25, 35]. It is straightforward to extend this scenario to other portals. The communication of the hidden sector with the MSSM is through kinetic mixing of the hidden photon, γ_d , of mass m_{γ_d} and the hypercharge field B_μ ,

$$\mathcal{L}_{mix} = \frac{1}{2}\epsilon\gamma_d^{\mu\nu}B_{\mu\nu} = \frac{1}{2}\epsilon\gamma_d^{\mu\nu}(\cos\theta_W A_{\mu\nu} - \sin\theta_W Z_{\mu\nu}) . \quad (2.1)$$

Here $\gamma_d^{\mu\nu}(B_{\mu\nu})$ is the field strength of $\gamma_d(B_\mu)$ and θ_W is the Weinberg angle. The mixing parameter, ϵ , is assumed to be small, $\epsilon \lesssim 10^{-3}$. The mixing with the photon can be removed by a shift of the photon field,

$$A_\mu \rightarrow A_\mu + \epsilon \cos\theta_W \gamma_d . \quad (2.2)$$

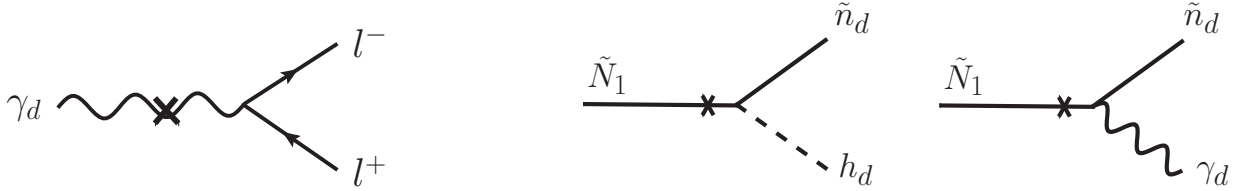


Figure 2: Interactions that follow from kinetic mixing between the hidden photon and hypercharge. The hidden photon couples to the electromagnetic current, including lepton pairs, as in the diagram on the *left*. The cross on the diagram indicates the ϵ suppression. The *right* two diagrams show possible decays of the SM bino to the hidden sector, which follow from gaugino kinetic mixing. The SM LSP is no longer stable, and all SUSY cascades can end in the hidden sector.

As a consequence, the hidden photon couples to all electrically charged particles with the strength $\epsilon e \cos \theta_W$. The smallness of ϵ implies millicharged couplings, consistent with all current bounds [33, 34]. The main significance of the above mixing is to trigger the decay of the hidden photon, γ_d , to kinematically accessible leptons and hadrons. This is illustrated with the left diagram of Fig. 2. Decays of the hidden photon to electrically neutral particles that couple to the Z , such as neutrinos, are suppressed by $m_{\gamma_d}^2/m_Z^2$ and will not play an important role. Similarly, we can ignore the mixing between the hidden and visible Higgses through the D-terms.

Upon supersymmetrizing Eq. (2.1), the hidden gaugino and visible bino (and therefore neutralinos) mix. One finds the kinetic mixing terms

$$-i\epsilon \tilde{\gamma}_d^\dagger \bar{\sigma}^\mu \partial_\mu \tilde{B} - i\epsilon \tilde{B}^\dagger \bar{\sigma}^\mu \partial_\mu \tilde{\gamma}_d. \quad (2.3)$$

Much as before, it is convenient to shift the hidden bino

$$\tilde{\gamma}_d \rightarrow \tilde{\gamma}_d + \epsilon \tilde{B}, \quad (2.4)$$

which removes the kinetic mixing, while keeping the mass matrix diagonal to order m_{γ_d}/m_Z . Consequently, hidden fields charged under $U(1)_d$ interact with the visible neutralinos with ϵ -suppressed couplings. In particular, all hidden sector scalars h_d^i , with charges q_i , couple to the visible bino,

$$- \epsilon g_d \tilde{B} \sum_i q_i h_d^{i\dagger} \tilde{h}_d^i. \quad (2.5)$$

Thus the visible neutralino may decay to the hidden neutralinos and either a Higgs or the longitudinal mode of the hidden photon, as in the right two diagrams of Fig. 2. In addition to the above, the small off-diagonal terms in the mass matrix induce m_{γ_d}/m_Z -suppressed couplings of the form

$$- \epsilon g' \frac{m_{\gamma_d}}{m_Z} \tilde{\gamma}_d \sum_i Y_i f^i \tilde{f}^i, \quad (2.6)$$

where $f^i(\tilde{f}^i)$ are MSSM (s)fermions, Y_i are the corresponding hypercharges, and g' is the hypercharge gauge coupling. This coupling will play a role in the sneutrino decay channel discussed in Section 3.2 below.

Finally, the hidden sector may have additional couplings to the visible sector. For instance, couplings of singlets in the superpotential,

$$W \supset S(y \chi \bar{\chi} + \lambda H_u H_d), \quad (2.7)$$

can lead to the *higgs portal*, $H_u H_d \chi^* \bar{\chi}^* + \text{c.c.}$, where χ and $\bar{\chi}$ are charged under the hidden sector. If χ and/or $\bar{\chi}$ get VEVs, this operator can trigger mixing between the MSSM Higgses and hidden particles. If $\chi, \bar{\chi}$ are relatively heavy the presence of the mixing does not change the decay branching fractions of the low-lying hidden states. The Higgs portal can, however, lead to Higgs decays into hidden sector particles. From now on we will refer to this mechanism as the *singlet channel*, which we return to in Section 3.3.

2.2 A Minimal Model

We now introduce the field content of a minimal hidden sector that leads to Higgs decays to lepton jets. In order to break the $U(1)_d$ gauge group, two Higgs chiral superfields, $h_{1,2}$ with charges ± 1 , are added. Generally, both Higgs fields obtain VEVs. This hidden sector setup was also studied in [15] (and we give further details in Appendix A). The hidden spectrum contains

- One massive photon γ_d ,
- Three hidden neutralinos \tilde{n}_d^i , which are mixtures of the hidden gaugino and Higgsinos,

- Three hidden scalars h_d^i : taking the hidden sector vacuum to preserve CP, there are two CP-even scalars, h_d, H_d , and one CP-odd scalar, A_d .

All these particles have masses which, for definiteness, are assumed to lie in the 100 MeV to few GeV ballpark. Supersymmetry is softly broken in the hidden sector, and we assume completely general soft and μ terms. This gives sufficient freedom to organize the masses in the hidden sector into various patterns leading to different types of cascades. The interactions within the hidden sector are fully dictated by gauge symmetry and supersymmetry. The neutralinos interact via,

$$\tilde{n}_d^i \tilde{n}_d^j h_d^k, \quad \tilde{n}_d^{i\dagger} \sigma_\mu \tilde{n}_d^j \gamma_d^\mu, \quad (2.8)$$

where the couplings are fixed by the hidden gauge couplings and mixing angles. Through these vertices the hidden neutralinos can cascade down to the lightest one (which we assume to be the true LSP¹, emitting hidden scalars and photons). Whenever it is kinematically available, the scalars can also decay through the vertices

$$h_d^i h_d^j h_d^k, \quad h_d^i \gamma_d^\mu (\gamma_d)_\mu, \quad (2.9)$$

that originate from the D-term and from the scalar kinetic terms.

Thus, depending on the mass spectrum, the cascades may lead to a large multiplicity of hidden particles in each event. The mass spectrum controls, for example, the typical length of the hidden cascade, the multiplicity of visible final states, and the amount of missing energy. The minimal model can be deformed by considering a non-Abelian hidden gauge group or by adding more chiral multiplets, both of which increase the number of scalar and fermionic eigenstates and can lengthen the hidden cascades, thereby producing a larger final state multiplicity. We study an example with such a modification in Section 7.3.

3 Higgs Decays to the Hidden Sector

The MSSM by itself allows for a rich variety of Higgs decay modes, depending on the visible spectrum. In particular, if the LVSP is sufficiently light, the Higgs can decay to it with

¹If visible-sector SUSY is broken by gauge mediation, there will also be a light gravitino. Hidden fermions decay to the gravitino well outside the detector [16], so here we can neglect the gravitino.

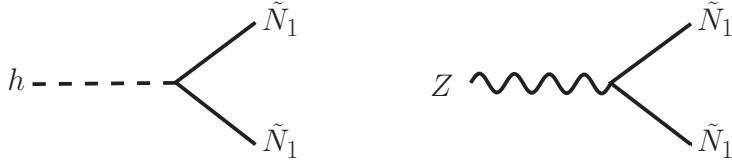


Figure 3: Higgs and Z decays to neutralinos. The neutralinos then decay into the hidden sector as in figure 2. We consider the region of the MSSM parameter space where the Higgs dominantly decays to neutralinos while the charginos are above the LEP bound of ~ 100 GeV. In this region, we find $m_{\tilde{N}_1} < m_Z/2$, such that the Z can also decay to neutralinos, as in the *right* diagram. This is consistent with LEP-1 constraints when $\text{BR}(Z \rightarrow 2\tilde{N}_1) \lesssim 10^{-3}$.

a sizable branching fraction, much larger than to the SM channels like $b\bar{b}$ or $\tau^+\tau^-$. If the LVSP is stable, such a scenario is strongly constrained by invisible Higgs searches at LEP [36]. The mixing of the hidden sector with the MSSM, however, makes the LVSP unstable. Then the Higgs can decay predominantly into complicated high-multiplicity final states. Such a possibility has not been experimentally studied at LEP or the Tevatron, therefore a priori a Higgs boson can be lighter than the naive LEP limit of 114.4 GeV. Below we identify three possible channels through which the lightest CP-even Higgs of the MSSM can decay into the hidden sector.

3.1 Neutralino Channel

In principle, there is no model-independent bound on the mass of the LVSP neutralino (this is because the bino is an MSSM singlet). The bounds on the Higgs boson mass can then be significantly relaxed, if the LVSP neutralino is sufficiently light, such that the Higgs branching fraction into it is $\gtrsim 75\%$, while a sizable fraction of the neutralino energy comes back in the form of visible SM states. A similar scenario with a light Hidden Higgs was considered in Ref. [10] within the R-parity violating MSSM, where the neutralino decays into three SM quarks, leading to the Higgs-to-6-jets signature. Higgs decays to neutralinos have also been considered in the framework of gauge mediation in [37]. Here we revisit the neutralino channel in the context of the Higgs decaying to lepton jets.

The coupling of the lightest MSSM Higgs boson to the lightest neutralino arises from the

Higgs-Higgsino-Bino/Wino couplings and takes the form,

$$g_{h11}h\tilde{N}_1\tilde{N}_1 + \text{h.c.}, \quad g_{h11} = \frac{1}{2}(gc_W - g'c_B)(c_\alpha c_U + s_\alpha c_D). \quad (3.1)$$

We parametrized the embedding of the lightest CP-even Higgs boson into the Higgs doublets as $H_u^0 = (s_\beta v + c_\alpha h + \dots)/\sqrt{2}$, $H_d^0 = (c_\beta v - s_\alpha h + \dots)/\sqrt{2}$. The angles c_i describe the composition of the lightest neutralino in terms of the original gauginos and Higgsinos: $\tilde{N}_1 = c_B\tilde{B} + c_W\tilde{W}^3 + c_U\tilde{H}_u^0 + c_D\tilde{H}_d^0$. The Higgs partial decay width is,

$$\Gamma(h \rightarrow \tilde{N}_1\tilde{N}_1) = \frac{g_{h11}^2 m_h}{4\pi} \left(1 - 4\frac{\tilde{m}_{N1}^2}{m_h^2}\right)^{3/2}. \quad (3.2)$$

This should be compared with the decay width into a pair of b -quarks,

$$\Gamma(h \rightarrow b\bar{b}) = c_{\text{QCD}} \frac{3}{8\pi} y_{hbb}^2 \left(1 - 4\frac{m_b^2}{m_h^2}\right)^{3/2}, \quad (3.3)$$

where $y_{hbb} = c_\alpha m_b/c_\beta v$ and c_{QCD} is a fudge factor that captures higher-order QCD effects. The latter are numerically relevant; for example, $c_{\text{QCD}} \approx 1/2$ for the SM Higgs of $m_h = 100$ GeV and for $m_b \approx 4.6$ GeV. The neutralinos then subsequently decay to the hidden sector through the couplings in Eq. (2.5). The decays are illustrated in Fig. 3.

Even if $m_{N1} < m_h/2$ (which is fairly easy to arrange) it is not automatic that the Higgs decays to neutralinos with a sizable branching fraction. Indeed, the coupling g_{h11} vanishes if the lightest neutralino is a pure gaugino or a pure Higgsino. The decays into neutralinos are therefore relevant only if the latter is a mixture of gauginos and Higgsinos. LEP constraints on a light SM Higgs require that

$$\Gamma(h \rightarrow b\bar{b})/\Gamma(h \rightarrow \tilde{N}_1\tilde{N}_1) \lesssim 0.25 \quad (3.4)$$

This is possible for example, if the lightest neutralino is dominantly a bino, with a 10% Higgsino fraction. A corollary is that the second visible neutralino and the lightest visible chargino cannot be arbitrarily heavy as otherwise the mixing angles $c_{U,D}$ would be suppressed. Thus there is tension between Eq. (3.4) and the LEP constraints on light charginos and the Tevatron constraints on trilepton signals from decays of the second to lightest neutralino².

²Although the standard supersymmetry searches are not necessarily sensitive to these models, we require the charginos to be heavier than the LEP reach ~ 100 GeV.

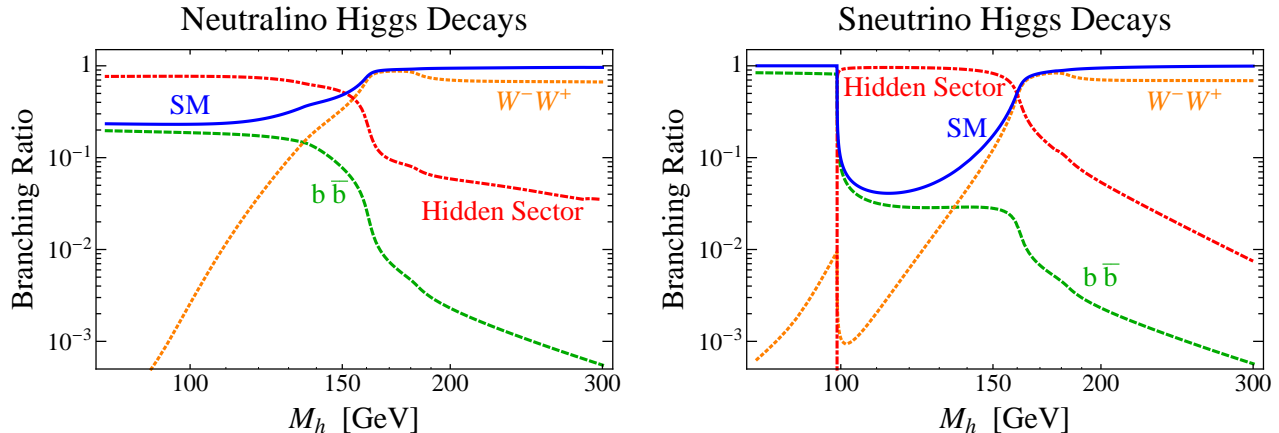


Figure 4: Higgs branching ratios for the neutralino and sneutrino channels. Each plot shows the total Higgs branching ratios to the SM and hidden sector, as functions of the Higgs mass. The SM width is dominated by the branching fractions to $b\bar{b}$ and W^+W^- , which are also shown separately. The parameters are fixed according to the benchmark models of Section 7.3. For each model, the Higgs decays dominantly to the hidden sector below the W^+W^- threshold, and a 100 GeV Higgs satisfies the LEP constraint $\text{BR}(h \rightarrow b\bar{b}) < 0.2$. The Higgs widths to SM states are taken from HDECAY [38].

Nevertheless, numerically one can find large portions of the parameter space where the Higgs decay into the lightest neutralino dominates, and at the same time the lightest chargino and the second neutralino are significantly heavier than 100 GeV, and thus beyond LEP reach. Trilepton constraints from the Tevatron, on the other hand, are model-dependent, because they depend on the branching fraction to trileptons and their kinematics. In Section 7.3, we will consider an example spectrum that is not constrained by trilepton searches.

Interestingly, all the viable points we have found correspond to the lightest visible neutralino mass below 40 GeV (this is consistent with the results of [10]). In consequence, the neutralino channel is constrained by LEP-1 searches (the Z boson can decay to neutralinos via its Higgsino component), but in the following we show that all existing experimental constraints can be satisfied. In the left plot of Fig. 4 we show the Higgs decay branching fractions as a function of the Higgs mass for the neutralino channel. The benchmark parameters of the specific model used are described in Section 7.3.

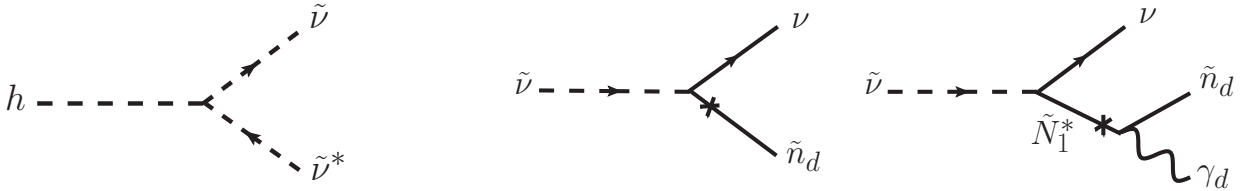


Figure 5: Diagrams relevant for Higgs cascade decays into the hidden sector via the sneutrino channel. The *left* diagram shows the Higgs decaying into a sneutrino pair. The *right* two diagrams are examples of two and three body decays of the sneutrino into hidden particles plus a SM neutrino. The neutrino production implies an irreducible missing energy component for this channel, which is constrained by LEP $h \rightarrow \cancel{E}_T$ searches, as discussed in Section 7.2.

3.2 Sneutrino Channel

The MSSM contains another class of neutral supersymmetric particles – the sneutrinos – which are the scalar partners of the SM left-handed neutrinos. If at least one of the sneutrinos is lighter than half the Higgs mass, another channel is open for the Higgs to decay into the hidden sector. In the MSSM, the Higgs couples to the sneutrinos through the $SU(2)_W \times U(1)_Y$ D-terms,

$$V_D \supset \frac{1}{8} (g'^2 + g^2) (|H_u|^2 - |H_d|^2 - |\tilde{\nu}_i|^2 + \dots)^2, \quad (3.5)$$

where $g'(g)$ is the hypercharge (weak) gauge coupling and the ellipses stand for additional terms which involve the sleptons and additional MSSM fields. The above term induces a tri-linear coupling between the lightest MSSM Higgs and two sneutrinos,

$$\frac{m_Z^2}{v} \sin(\alpha + \beta) h \tilde{\nu}^\dagger \tilde{\nu}, \quad (3.6)$$

where the resulting Higgs decay width is

$$\Gamma(h \rightarrow \tilde{\nu}\tilde{\nu}) = \frac{m_Z^4}{16\pi m_h v^2} \sin^2(\alpha + \beta) \left(1 - 4\frac{m_{\tilde{\nu}}^2}{m_h^2}\right)^{1/2}. \quad (3.7)$$

The Higgs-sneutrino coupling is typically large, thus the $h \rightarrow \tilde{\nu}\tilde{\nu}$ decay normally dominates over $h \rightarrow b\bar{b}$ as soon as it is kinematically allowed. This is shown in the right plot of Fig. 4 for the benchmark model described in Section 7.3. The sneutrino cannot be lighter than $m_Z/2$ as this is excluded by the LEP-1 measurement of the Z -width. This leaves the window

$m_Z/2 < m_{\tilde{\nu}} < m_h/2$ where the decay into sneutrinos can potentially lead to a hidden and light Higgs.

Much as in the neutralino LVSP case, the sneutrino is not stable and hence the Higgs decaying into sneutrinos is not invisible. There are two ways for the sneutrino to decay into the hidden sector, both illustrated in Fig. 5. Since the bino is heavy in this scenario, Eq. (2.6) induces a three-body decay into a neutrino, a hidden neutralino and a hidden boson (scalar or photon). Conversely, the sneutrino can decay directly into a SM neutrino and a hidden neutralino, through the interaction in Eq. (2.6), however, the coupling is suppressed by an additional $m_{\tilde{\gamma}_d}/m_Z$ factor. As a consequence, the 3-body decay is dominant, unless the lightest visible neutralino is significantly heavier than 100 GeV. The sneutrino decay may be followed by a cascade in the hidden sector leading to a final state with a number of visible leptons and missing energy from the true LSP in the hidden sector. Due to the SM neutrino in the final state, the sneutrino channel is characterized by more missing energy than the neutralino channel.

As we will discuss below, the sneutrino channel, together with the minimal $U(1)_d$ hidden sector of Section 2.2, suffers from considerable tension with several LEP searches. Two reasons are the typically larger missing energy in the Higgs decays through the sneutrino channel and the independent sneutrino production cross-section through off-shell Z 's, which is comparable in rate to Higgs-strahlung. An extended hidden sector, with additional cascades, can resolve this tension. We return to these issues in Section 7.

3.3 Singlet Channel

Finally, new Higgs decay modes are possible, if there are additional mediators that couple both to the Higgs and to the hidden sector. A simple example is constructed starting from the NMSSM in which an additional singlet, S , couples to the Higgs doublets. S obtains a VEV, thereby ameliorating the so called μ -problem. To enable the Higgs decays, consider, as an example, the following superpotential,

$$W_{\text{singlet}} = S (y \chi \bar{\chi} + \lambda H_u H_d) + \kappa_1 \bar{\chi} h_1^2 + \kappa_2 \chi h_2^2. \quad (3.8)$$

Here $\chi, \bar{\chi}$ are chiral superfields with charges ± 2 under G_d and $h_{1,2}$ are the two hidden Higgses. Once the visible Higgses and the singlet acquire VEVs, masses for $\chi, \bar{\chi}$ are generated: the

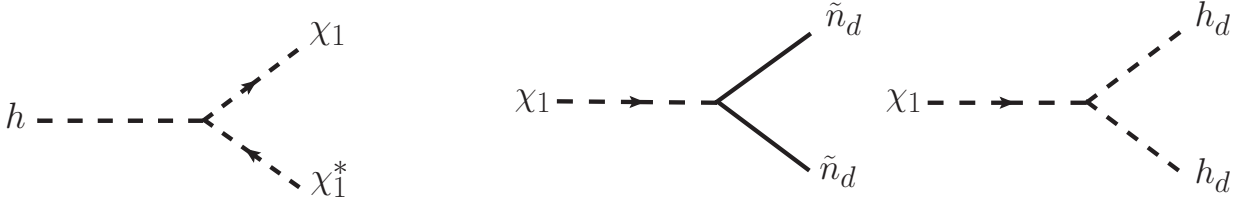


Figure 6: Diagrams relevant for Higgs cascade decays into the hidden sector via the singlet channel of Eq. (3.8). The scalars that couple to the Higgs are split by the NMSSM singlet F -term, such that the lighter one, χ_1 , is easily lighter than half the Higgs mass. The scalars couple to light hidden sector Higgses through the superpotential, and the *right* two diagrams are examples of the resulting decays of χ_1 into hidden fermions and scalars.

fermionic degrees of freedom get a mass $y\langle S\rangle$, while the scalar masses are split by the F -term of S , $m_\chi^2 = y^2\langle S\rangle^2 \pm y F_S$. If the lightest scalar state is lighter than $m_h/2$, the Higgs can decay into a pair of these fields with a large branching fraction, as long as the couplings y and λ are sizeable. Quite generically, the branching fraction into the hidden sector is close to unity. The branching fraction for the benchmark model described in Section 7 is shown in the right plot of Fig. 7.

Subsequently, the χ states decay via the $\kappa_{1,2}$ couplings into hidden Higgsinos and Higgses, which finally decay to SM fermions. Once again the final state of the Higgs decay is a number of leptons plus missing energy. The virtue of this model is that it requires a minimal deformation of the NMSSM (or other variants which address the μ -problem), and is by and large independent of the visible spectrum. It can therefore accommodate heavy SM superpartners which are beyond the LEP and Tevatron reach, while allowing the Higgs to decay dominantly into the hidden sector. Such a model is therefore in principle less constrained by existing searches.

4 Collider Phenomenology

In order to establish models where the Higgs and possibly SUSY are hidden, we must understand how the phenomenology of this scenario is experimentally constrained. In this section, we describe the collider physics of a Higgs decaying to lepton jets. We begin, in Section 4.1, with a general description of lepton jets and neutralino jets, which are a particular subclass

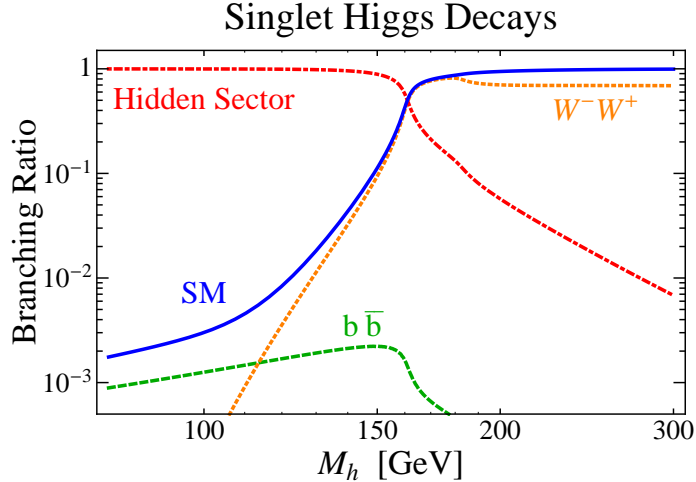


Figure 7: Same as in Fig. 4, for the singlet channel, with the parameters fixed according to the benchmark of Section 7.3.

defined below. Then, in Section 4.2, we describe the most prominent experimental variables of this scenario, defining a space of observables. After discussing the relevant LEP and Tevatron searches in Section 6, we continue in Section 7 by identifying the allowed region in this space of experimental observables. We then construct benchmark models that reside in this allowed region.

4.1 Lepton Jets and Neutralino Jets

The Higgs can avoid detection at LEP and the Tevatron if it decays into final states that are relatively unconstrained by existing searches. Here we focus on one such class of final state objects: *lepton jets*, which are defined as high-multiplicity clusters of boosted and collimated leptons [14, 15, 16]. Lepton jets can be produced when the Higgs decays through low lying hidden sector states with masses (in particular the hidden gauge boson) below $\lesssim 1$ GeV. These hidden sector states then decay to leptons. The picture is the following. First, the Higgs boson is produced, alone or in association with Z or W , and decays into a pair of SM superpartners or singlets. We discussed three such channels in Section 3. The pair promptly decays into the hidden sector, cascading through hidden sector interactions to produce highly boosted hidden scalars, photons and neutralinos. These appear in the

detector either as missing energy or produce boosted leptons which populate lepton jets. An example of such a Higgs cascade decay is depicted in Fig. 1.

The number of lepton jets per Higgs decay depends on the cascading spectrum, and the resulting topology is easily deduced by recalling that particles produced at rest decay to well-separated objects while boosted particles decay to collimated objects. For example, if the Higgs decays to two weak scale SM superpartners or singlets, each will decay to well-separated hidden particles that seed distinct lepton jets. Subsequent decays will be collimated, and the event topology can contain as many as four lepton jets. Alternatively, for example, if the Higgs decays to two very light neutralinos, $m_{\tilde{N}_1} \lesssim 10$ GeV, then each neutralino's decay products will be clustered, and the event topology will contain two lepton jets, one for each neutralino. In this situation, we refer to the lepton jets as *neutralino jets*. We consider an example with neutralino jets in Section 7.3.

4.2 Experimental Observables

Concentrating on the lepton jets, we identify the following relevant collider variables,

- **Visible Final States: Electrons vs. Muons**

The hidden photon decays through the kinetic mixing, Eq. (2.1), into all kinematically allowed SM states with electric charge. Thus, the mass of the hidden photon is the only parameter controlling which visible particles appear at the end of the Higgs cascade decay. For $m_{\gamma_d} < 2m_e$ the hidden photon is stable on collider scales, which would amount to a purely invisible Higgs signature. This scenario is strongly constrained, as we review in Section 6, and we do not consider this possibility here. For $2m_e < m_{\gamma_d} < 2m_\mu$ the hidden photon decays exclusively into electrons. For $2m_\mu < m_{\gamma_d} < 2m_{\pi^\pm}$ the hidden photon decays into a pair of muons or electrons, roughly in equal amounts. For $m_{\gamma_d} > 2m_{\pi^\pm}$ the branching fractions are determined by $R \equiv \text{BR}(e^+e^- \rightarrow \text{had})/\text{BR}(e^+e^- \rightarrow \mu^+\mu^-)$ [39, 33] which is measured experimentally [40]. As long as $m_{\gamma_d} \lesssim 400$ MeV, $\text{BR}(\gamma_d \rightarrow \pi^+\pi^-)$ is less than 10% and can be safely neglected, as we do below. The branching fractions are shown in Fig 8.

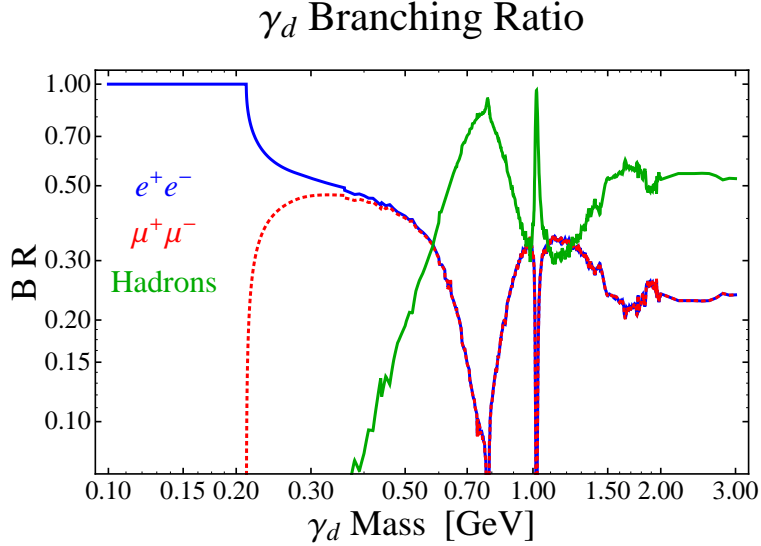


Figure 8: Hidden photon branching ratios to electrons, muons, and hadrons through the electromagnetic current, as a function of the hidden photon mass. The hadronic branching ratio is derived from the measured $R \equiv \text{BR}(e^+e^- \rightarrow \text{had})/\text{BR}(e^+e^- \rightarrow \mu^+\mu^-)$ [40]. We see that for $m_{\gamma_d} \lesssim 500$ MeV, the hidden photon decays dominantly to leptons, including muons for $m_{\gamma_d} > 211$ MeV.

- **Lepton Multiplicity**

This observable is extremely sensitive to the details of the hidden sector spectrum. One important factor is the identity of the lightest hidden neutralino. Since the visible bino couples to hidden Higgsinos, see Eq. (2.5), model realizations where the hidden bino is lighter than the hidden Higgsinos have longer cascades, and therefore tend to produce more visible leptons. Another crucial factor is the ratio of the masses of the lightest hidden scalar and hidden photon. When $m_{h_d} < m_{\gamma_d}$, the hidden Higgs, h_d , dominantly decays to 2 leptons at one-loop [33], and is stable on collider scales. On the other hand, for $m_{h_d} > m_{\gamma_d}$ the 3-body decays with one on-shell hidden photon are allowed, which leads to prompt decays of h_d into 4 leptons, as long as the mixing parameter ϵ is not too small. The spectrum of the other hidden scalars is also important. For example, when $m_{H_d} > 2m_{h_d}$ the dominant decay mode of H_d is $H_d \rightarrow 2h_d \rightarrow 8l$, while for $m_{\gamma_d} < m_{H_d} < 2m_{h_d}$ the 4-lepton decay via the hidden photons dominates. Depending on the mass spectra, the average lepton multiplicities can thus range from zero to a few

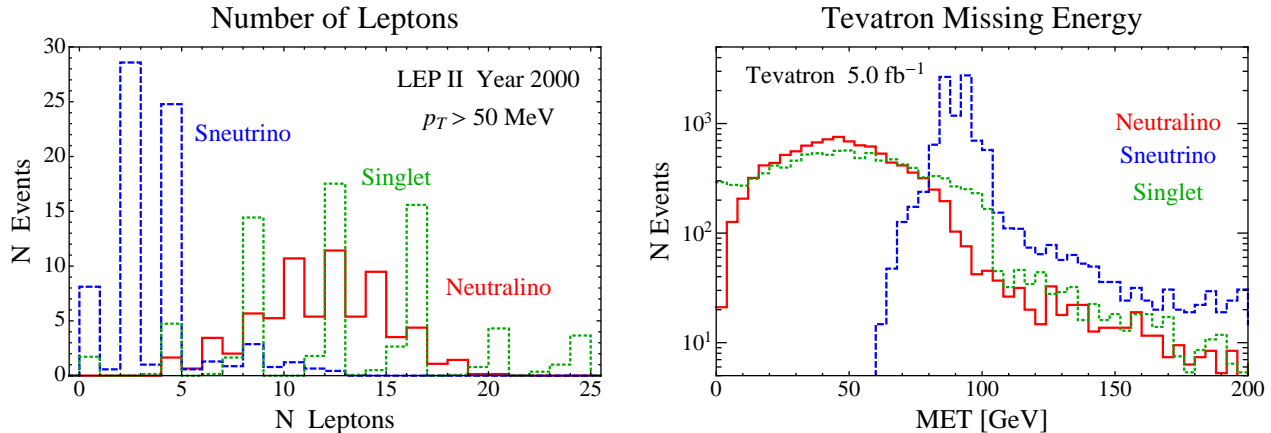


Figure 9: The lepton multiplicity and missing transverse energy distributions of Higgs decays for the three benchmarks of section 7.3. The *left* panel shows the multiplicity of leptons with $p_T > 50$ MeV, which is roughly the threshold for detecting tracks at LEP. The event counts correspond to the data collected in the year 2000 at LEP-2, corresponding to $\mathcal{L} \approx 214$ pb⁻¹ at $\sqrt{s} = 205 - 207$ GeV. The *right* panel shows the missing energy distribution at Tevatron Run II, $\sqrt{s} = 1.96$ TeV, and the event counts correspond to $\mathcal{L} = 5$ fb⁻¹. The sneutrino benchmark has the most missing energy because of the irreducible missing energy carried by the neutrinos.

tens of leptons per Higgs decay. Going beyond the minimal $U(1)_d$ model, for example by making the hidden group non-Abelian, only increases the number of possibilities. Additionally, if the hidden gauge coupling is sizeable ($g_d^2/4\pi \gtrsim 0.1$), hidden sector showering also increases the number of leptons [39, 15]. Example lepton multiplicity distributions are given in Fig. 9.

- **Missing Energy**

The average missing energy per Higgs decay is also very sensitive to the hidden spectrum. The missing energy can range anywhere from being very small, less than 10 GeV, to where it dominates over visible energy. The most important factor determining the amount of missing energy is how many hidden particles are collider-stable. Furthermore, missing energy depends on the Higgs decay channel into the hidden sector. For the sneutrino channel the amount of missing energy is typically larger, because a hard neutrino is emitted when the sneutrino decays into the hidden sector. For typical hidden spectra the average missing transverse energy per Higgs decay is on the order of 10-50 GeV, and displays a large variation on an event-by-event basis, see Fig. 9.

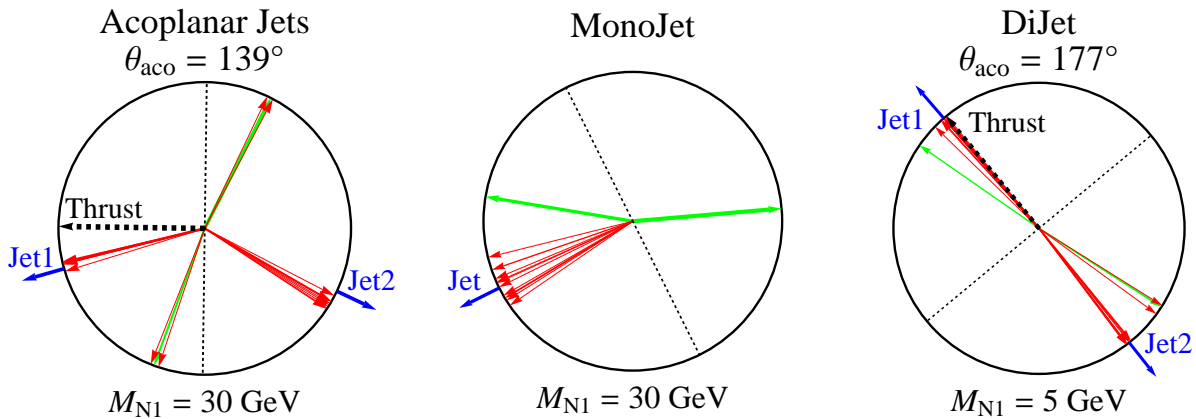


Figure 10: Transverse event displays for Z decays to neutralinos at LEP-1. The red vectors show the transverse momenta of leptons and the green vectors correspond to long-lived hidden sector particles that escape the detector as missing energy. The *left* display shows a 4-lepton-jet event, with $m_{\tilde{N}_1} = 30$ GeV, that would have been detected by the ALEPH acoplanar jet search [41]. The thrust (black) is used to define two jets (blue). In an acoplanar event, the jets are separated by $\theta_{\text{aco}} < 175^\circ$ in the transverse plane. The *central* display shows an event that would have been detected by the ALEPH monojet search [42] because all visible energy falls in the same hemisphere. Here, both neutralinos produce exactly one visible lepton jet in the same hemisphere, balanced by missing energy. Both acoplanar jets and monojets are avoided if $m_{\tilde{N}_1} \lesssim 5$ GeV with both neutralinos decaying (partly) visibly, as in the *right* display. The topology of the back-to-back neutralino jets mimic the hadronic dijet background.

- **Event Topology: Number of Lepton Jets**

The directions of final state lepton momenta are not distributed randomly. Hidden sector particles are produced with large boosts, and their clustered decay products populate distinct lepton jets containing highly collimated leptons. The final state topology is characterized by the number of lepton jets, which depends on the spectrum and first steps of the cascade decay. A two-jet topology arises when the Higgs decays directly into two GeV scale objects, or if the superpartners decay into one hidden particle that decays visibly along with other invisible particles. The former possibility is most easily realized with the neutralino jets discussed in Section 4.1. Indeed, if the lightest MSSM neutralino mass is below 10 GeV (which is possible without compromising naturalness, and without conflicting experiment), its visible decay products

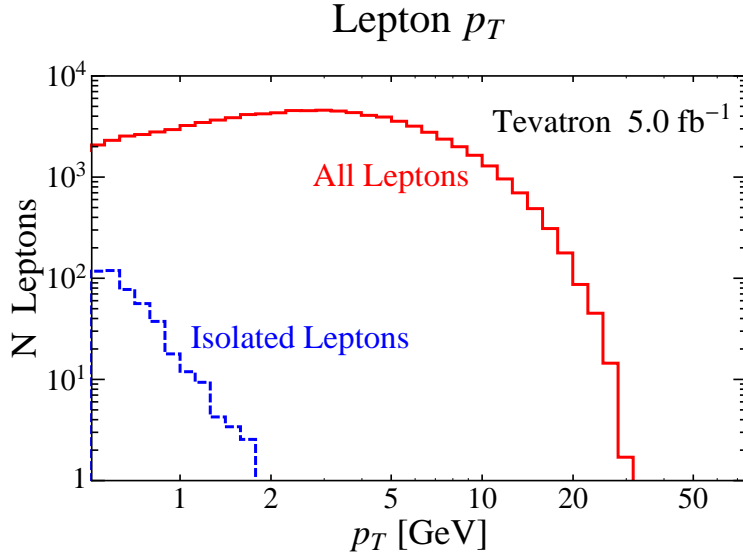


Figure 11: The p_T distributions of all leptons (solid, red) and isolated leptons (dashed, blue) produced in gluon fusion Higgs decays at Tevatron Run II, $\mathcal{L} = 5 \text{ fb}^{-1}$, for the singlet benchmark of section 7.3. Tevatron searches for trileptons and like-sign dileptons impose strict isolation requirements in order to fight the SM heavy flavor and in-flight-decay backgrounds. For this plot, we use a track-based isolation definition where the scalar p_T sum of all other tracks in a cone surrounding the lepton, $\Delta R < 0.4$, must not exceed 10% the p_T of the lepton [43]. We see that Higgs decays to lepton jets produce few isolated leptons, all of which are soft.

form a jet along its direction of motion. On the other hand, when the Higgs decays into neutralinos heavier than 10 GeV, or when the three-body decays of the sneutrino channel dominate, the event topology will contain 3 or more jets. Finally, if one of the two primary Higgs decay products (neutralinos, sneutrinos or hidden fields) decays invisibly, while the other decays into one lepton jet, the final state will display a monojet topology. All three possibilities are shown in Figure 10.

- **Lepton Isolation**

Yet another consequence of their boosted origin is that lepton jets are narrow, with constituent leptons that are not isolated. Tevatron searches for new physics that produces leptons, such as the trilepton and like-sign dilepton searches discussed in Section 6.3, require isolated leptons in order to fight the backgrounds from heavy-flavor decays and in-flight meson decays. These searches typically require leptons to be isolated

within cones of $\Delta R < 0.4$. Some searches require total isolation in this cone [44], while other searches put limits on the energy deposition in the calorimeters [45], or the sum of track p_T [43]. Lepton jets violate these isolation definitions because each hidden photon decays into a pair of close leptons separated by $\Delta R \lesssim 0.1$. Thus, almost all leptons in the final state have at least one companion track within the isolation cone³. Furthermore, the bulk of our parameter space leads to large lepton multiplicities with numerous leptons in a $\Delta R \sim 0.1$ cone, further spoiling the isolation. In Fig. 11 we show the distribution of the total number of leptons as a function of the transverse momenta together with leptons that satisfy the track-based isolation of Ref. [43]. One can see that only a small fraction of the leptons are isolated, and these are typically soft leptons that would not pass the p_T cuts for most new physics analyses. The other isolation definitions give similar results.

- **Displaced Vertices**

A final feature of this class of models is the possible existence of displaced vertices. For instance, displaced vertices are produced if the kinetic mixing, ϵ , is small enough. The hidden photon decay length scales as $1/\epsilon^2$, so that for hidden photon mass $m_{\gamma_d} \simeq 0.1$ GeV, displaced vertices show up for $\epsilon \lesssim 10^{-5}$. Displaced vertices can also appear for a subset of final state particles, in three-body decays, if mass splittings in the hidden sector are small compared to the GeV scale. This can occur without tuning. For example, the splitting between two hidden neutralinos can be naturally small if they are both Higgsino-like. The presence of displaced vertices would avoid most of the existing LEP and Tevatron constraints, as such signal events would not be selected by most analyses. Higgs decays with displaced vertices were studied in [28, 46]. To keep our discussion simple we do not consider them in this paper. Nonetheless, one should keep in mind that this possibility could be realized in nature and would relax the constraints on new physics. Conversely, designing collider search strategies that would be sensitive to a Higgs decaying to lepton jets with displaced vertices is an important

³Isolated leptons are sometimes produced when soft leptons are emitted at wide angles from the rest of the lepton jet or when nearby leptons are too soft to reach the calorimeter (e.g. $p_T \leq 0.5$ GeV at Tevatron), and are therefore interpreted as missing energy.

task that we postpone for future work.

5 Can Lepton Jets Really Hide the Higgs?

Before considering specific searches, it is natural to ask whether Higgs decays to lepton jets would have been trivially seen at LEP and/or the Tevatron. In other words, one might think that it is naive to imagine that such spectacular events can remain undetected. To address this worry let us first consider LEP-2, which sets the strongest limits on a light Higgs. The production cross-section, for a 100 GeV Higgs, is around $0.3 - 0.4$ pb. The total luminosity at LEP-2 is on the order of 450 pb^{-1} , per experiment. The number of Higgs-strahlung events before cuts is therefore ~ 130 . Preliminary cuts typically reduce the number of events by an order of magnitude, leaving only a handful of events and making detection nontrivial without a dedicated search. Furthermore, due to the relatively poor quality of the hadronic calorimeters at the LEP experiments, hadronic activity is typically identified by the number of tracks. For this reason, even at LEP-1 where the neutralino channel allows for as many as 10^4 lepton jet events, these events are easily hidden beneath the large hadronic background.

At the Tevatron, Higgs production is dominated by gluon fusion with a cross-section of ~ 2 pb for a 100 GeV Higgs. With 5 fb^{-1} this implies 10^4 Higgs events. Of course, the large QCD background does not allow one to search for such events ‘by eye’. Even so, one may worry that the existence of many leptons would, naively, allow for an easy discovery. The key point is that Tevatron searches for leptons require them to be isolated. This is true, in particular, for the Vista/Sleuth global searches which take a model-independent approach [47]. The leptons produced by Higgs decays to lepton jets are typically not isolated, and thereby evade the standard searches. The small number of Higgs events that do produce isolated leptons are buried beneath the QCD and electroweak backgrounds.

6 Experimental Constraints

The strongest constraints on the Higgs mass and decay branching fractions come from LEP-2 searches. These are obtained assuming the Higgs is dominantly produced through the Higgs-strahlung process, $e^+e^- \rightarrow Zh$, with the SM cross section. Three well known results

should be kept in mind:

1. The most robust constraint on the Higgs mass comes from the model independent search by OPAL [13], $m_h \geq 82$ GeV. This bound is independent of the Higgs decay modes.
2. The mass of the SM Higgs is constrained to be $m_h \geq 114.4$ GeV [48]. This bound is obtained by studying the dominant $h \rightarrow b\bar{b}$ SM decay. Conversely, the study can be interpreted as a bound on the $h \rightarrow b\bar{b}$ branching ratio, which for a 100 GeV Higgs is bounded to be $\text{BR}(h \rightarrow b\bar{b}) \lesssim 20\%$ [4].
3. Finally, the invisible Higgs (where the Higgs decays exclusively into missing energy) must be heavier than 115 GeV [49]. Again, the bound can be interpreted also as the bound on the branching ratio of Higgs to invisible states. For a 100 GeV Higgs the bound is $\text{BR}(h \rightarrow \cancel{E}) \lesssim 15\%$.

The LEP collaborations have performed several searches for Higgs decaying into 2 SM particles other than the b quarks, always placing a bound on the Higgs mass almost as stringent as the SM one, see [5] for a review. Higgs decaying into a larger number of SM states is considerably less constrained, with the exception of $h \rightarrow 4b$ and $h \rightarrow 4\tau$ channels. Thus, Higgs decaying into high multiplicity final states offers a way to circumvent the LEP limits, as long as 2-body decay channels are sufficiently suppressed.

Higgs decaying to lepton jets has not been searched for at LEP or the Tevatron. In this scenario the Higgs mass is in principle constrained only by the OPAL model-independent limit. But the final states predicted by this scenario could well be picked up by some existing Higgs or new physics searches. This section provides an overview of the most relevant searches at LEP and the Tevatron together with a brief explanation why they could be sensitive to the Higgs decaying to lepton jets.

6.1 LEP-1 Searches

The LEP-1 searches are relevant for the neutralino channel, Section 3.1, because in this scenario the lightest MSSM neutralino is necessarily lighter than $m_Z/2$ [10]. The Z boson

can then decay into a pair of neutralinos, each of which decays via the hidden sector cascade into a hidden neutralino and lepton jets. Even though $BR(Z \rightarrow \tilde{N}_1 \tilde{N}_1)$ can be as small as $10^{-3} - 10^{-4}$, this still leaves $10^3 - 10^4$ neutralino/lepton jets at LEP-1. For the sneutrino channel, Section 3.2, the measurement of the Z width at LEP-1 constrains the branching ratio of Z into any new particle to be smaller than 10^{-3} [50]. This immediately implies $m_{\tilde{\nu}} > m_Z/2$. For the singlet channel, Section 3.3, the LEP-1 searches are not important since the hidden fields do not couple to Z at leading order.

We have identified the following searches that could be sensitive to $Z \rightarrow \tilde{N}_1 \tilde{N}_1 \rightarrow$ lepton jets + \cancel{E} decays in our scenario

- **Monojets**

In [42] the ALEPH collaboration analyzed the so-called monojet events where no energy is detected in the hemisphere opposite to the direction of the total visible momentum. This can happen, if the neutralinos are produced at rest or in those corners of the parameter space where the hidden cascade yields a low multiplicity of visible states, in particular, if one of the neutralinos decays invisibly. Conversely, these constraints are typically avoided, if the neutralino decays to a large number of visible states.

- **Acoplanar Jets**

Events can be clustered into two jets by summing the total momenta in each of the two hemispheres defined by the plane perpendicular to the thrust axis. Acoplanar jets are then defined by requiring that the angle between transverse momenta of the two jets is smaller than, e.g., 175° [41]. In Ref. [41] the ALEPH collaboration searched for acoplanar jets accompanied by missing energy. The signal events often contain a large number of charged tracks (especially if the model satisfies the monojet constraints). Therefore they may be efficiently picked up by this analysis, even though it was designed to search for hadronic events.

- **Energetic Lepton Pairs**

Also in Ref. [41], ALEPH made a search for energetic lepton pairs in hadronic events. In the neutralino channel, Section 3.1, two of the multiple leptons from the neutralino jet can readily meet the definition of the energetic pair.

6.2 LEP-2 Searches

The following LEP-2 Higgs searches are sensitive to the events $e^+e^- \rightarrow Zh$ with $h \rightarrow$ lepton jets + \cancel{E} and could potentially constrain our scenario.

- **Flavor-independent Higgs**

LEP has constrained the Higgs boson decaying into generic jets without relying on b -tagging. These searches can be relevant since our signal often displays a two-jet topology. The analysis of the OPAL collaboration [51] is the most straightforward to interpret in our framework, because it does not rely on neural network techniques. However the presence of missing energy makes the $H \rightarrow 2j$ searches less sensitive to the signal, as compared for example with the squark searches described later in this subsection.

- **Invisible Higgs**

Searches for the Zh final state where h decays entirely into missing energy have been performed by all collaborations [49]. The most relevant for us is the OPAL invisible Higgs search [36], because its visible mass cut is the least aggressive, $50 \text{ GeV} < M_{\text{vis}} < 120 \text{ GeV}$. This search can strongly constrain our models, especially the sneutrino channel where the invisible energy fraction is typically larger due to the neutrinos produced by sneutrino decays. This search can also pick up the signal events in the case of the neutralino and the singlet channel models, if the associated Z boson decays invisibly.

- **Higgs to WW^***

In Ref. [52] the ALEPH collaboration performed a search for $h \rightarrow WW^*$ decays in the context of fermiophobic Higgs models. Leptonic decays of W lead to final states with electrons/muons and missing energy, so that the ALEPH search targets final states similar to our signal — lepton jets and missing energy. Furthermore, the data sample is systematically divided into distinct classes corresponding to different decay topologies of the WW^* system. The $h \rightarrow WW^*$ search thus turns out to be very sensitive to Higgs decaying to lepton jets.

- **Higgs to 4τ**

Very recently, an analysis of the $h \rightarrow AA \rightarrow 4\tau$ decay was presented by the ALEPH collaboration [12]. This search targets the case where the intermediate pseudoscalar A is very light, 10 GeV or less, in which case Higgs decays into two pairs of nearly overlapping τ^\pm . Since tau leptons decay into 1 or 3 charged particles most of the time, the analysis focuses on 2-jet events that contain 2 or 4 tracks per jet, while the associated Z is assumed to decay invisibly or leptonically. From our perspective, the analysis is very relevant, since no τ identification is attempted, other than constraining the number of tracks. Therefore, Higgs-to-lepton jets signal might be picked up, if the Higgs decays to a small enough number of charged states.

Apart from the Higgs searches, certain SUSY searches could also be sensitive to the Higgs-to-lepton jet final state,

- **R-parity Violation**

If there is R-parity violating operator LLE^c in the superpotential, the lightest neutralino or sneutrino decay to leptons and neutrinos. In that context, ALEPH [53] and DELPHI [54] analyzed final states with multiple leptons and missing energy.

- **Six-Leptons**

Multilepton final states can also arise from slepton decays in (R-parity conserving) gauge mediated SUSY breaking scenarios, where the missing energy is carried away by a gravitino. The ALEPH search for 6 lepton final states is described in Ref. [55].

- **Squark Searches**

Squark pair production at LEP can lead to a final state with two acoplanar jets, where each jet has small invariant mass, accompanied by missing energy (and possibly additional leptons). The searches of OPAL [56] and ALEPH [57] can pick up the signal when the Higgs decays to lepton jets carrying a large number of leptons, while the associated Z decays invisibly. The OPAL search turns out to be especially constraining, due to the fact that the number of observed events is well below the expected SM background.

6.3 Tevatron Searches

The Tevatron experiments search for lepton jets in a noisier hadronic environment. Even so, due to the large Higgs production cross-section and the high luminosity, discovery may be within reach with possibly many light Higgs-to-lepton jets events already on tape. We identify the following relevant searches⁴

- **Dark Photon Search**

Recently, the D0 collaboration has made a search [59] for hidden photons produced in neutralino decays. In addition to the lepton jet, a requirement for an isolated (ordinary) photon is made. The photon requirement reduces significantly the expected signal from Higgs-to-lepton jets decays, where the photon can come only from initial state radiation. In addition, the D0 search requires the lepton jet to have only two leptons which is uncommon in our scenario.

- **NMSSM Hidden Higgs**

Ref. [60] targeted a Higgs boson decaying into 4μ and $2\tau 2\mu$ final states via an intermediate pair of pseudoscalar singlets of the NMSSM. The search focused on the case where the pseudoscalar is fairly light, so that the muon and tau pairs to which it decays are highly collimated. Consequently, Ref. [60] looked for isolated muons with close companion tracks. This topology can readily arise in Higgs-to-lepton jet decays as long as the hidden photon is heavy enough to decay into muon pairs.

Studies of multilepton final states have been routinely performed at the Tevatron, mostly in the context of SUSY searches. The SM processes are unlikely to produce 3 or more energetic and *isolated* leptons, therefore such topologies offer clean channels to search for new physics. Although these searches typically target isolated high- p_T leptons, it is conceivable that a subset of our signal events may yield muons and electrons passing the selection criteria. The most interesting from our perspective are

⁴Multilepton signatures were also addressed in Ref. [58] where an excess of multi-muon events was reported. This search focuses on events with displaced vertices, and therefore it is not relevant for the Hidden Higgs signal we consider in this paper. In any case, cross sections required to address the CDF multi-muon excess are orders of magnitude larger than the Higgs production cross section at the Tevatron.

- **Trilepton Searches**

Of all trilepton searches Ref. [44] is singled out because it is based on the largest data sample of 3.2 fb^{-1} . Moreover, the cuts on lepton p_T and on missing transverse energy are relatively soft. However, the isolation requirements are quite severe. In particular, all objects in the analysis are required to be separated by $\Delta R > 0.4$, which decreases the sensitivity to the Higgs-to-lepton jets signal. Another search in Ref. [45] focused on di-muon pairs accompanied by a third lepton with a very low p_T threshold of 5 GeV. In this case lepton isolation is determined by calorimeter deposits: less than 10 percent of the lepton p_T should be detected in the $\Delta R = 0.4$ cone around the lepton.

- **Like-Sign Dilepton Searches**

Ref. [43] focused on events with two energetic electrons or muons of the same electric charge and large invariant mass. Such a pair can arise in the signal when the two selected leptons come from separate lepton jets, or when a lepton in a lepton jet is paired with another lepton from W or Z decays. Again the sensitivity to our signal is reduced by the isolation requirements: the sum of the transverse energy within $\Delta R = 0.4$ around the leptons must be less than 10 percent of the lepton p_T .

7 Hiding the Higgs

In this section we discuss the implications of the experimental searches, listed in Section 6, for viable models where the Higgs decays dominantly to lepton jets. After introducing our methodology in Section 7.1, we show in Section 7.2 that the set of observables (listed in Section 4.2) are constrained by LEP and the Tevatron, to a particular region which can accommodate a light Higgs decaying to lepton jets. In Section 7.3 we then present concrete benchmark models that hide the Higgs.

7.1 Methodology

We are interested in how well the LEP and Tevatron searches listed in Section 6 constrain the Higgs decaying to lepton jets. No searches have explicitly placed limits on this signal, thus the limits must be inferred from simulation. We simulate Higgs production and decays

to lepton jets using Monte Carlo and evaluate the efficiency of the above searches by making the appropriate cuts on the produced signal events. We use `Madgraph` [61] to simulate the Higgs production and decay into the hidden sector, `BRIDGE` [62] to simulate the hidden sector cascades that populate lepton jets, `Slowjet` [63] for event analysis, including kinematic cuts, jet clustering, and lepton isolation. We do not simulate hidden sector showering, which can be important for $g_a^2/4\pi \gtrsim 0.1$ [15, 39]. It is important to keep in mind that, due to the collimated nature of lepton jets, some tracks may fail to reconstruct and some leptons may fail lepton identification. While we work with the ideal situation where this is not the case, but to set reliable limits on scenarios where the Higgs decays to lepton jets, a more comprehensive study with full detector simulation is necessary. Such a study is beyond the scope of this paper.

7.2 Constraints on Experimental Observables

We now discuss how the experimental searches constrain viable Higgs-to-lepton jets signatures. We consider the observables: event topology, lepton multiplicity, lepton species, and missing energy listed in Section 4.2. The discussion includes all three production channels discussed in Section 3.

We begin by arguing that several searches lead one to consider a two-jet topology for the lepton jets. For instance, the neutralino channel is strongly constrained by the acoplanar jet search at LEP-1 [41], where neutralino pairs can be produced in rare Z decays. While constraints on the Z -width allow the Z branching fraction to neutralinos to be as large as 10^{-3} , the branching fraction to 3 or more lepton jets must be suppressed by $\sim 10^{-6}$ in order for the model not to be excluded. Such low branching ratios are obtained for a very light neutralino, $m_{\tilde{N}_1} \lesssim 5$ GeV, where the resulting event topology consists of two back-to-back neutralino-jets (shown in the third panel of Figure 10). Decays with such a topology are not excluded because of the kinematical similarity to the large hadronic Z background. A two-jet topology is also favored by the $h \rightarrow WW^*$ search at LEP-2 [52]. Especially constraining is a search subclass consisting of a final state with two hard leptons, ($E_T > 25$ GeV and $E_T > 20$ GeV), a softer lepton ($E_T > 8$ GeV), and at least two additional tracks. This selection has a small SM background, which is further reduced by using the Durham jet clustering

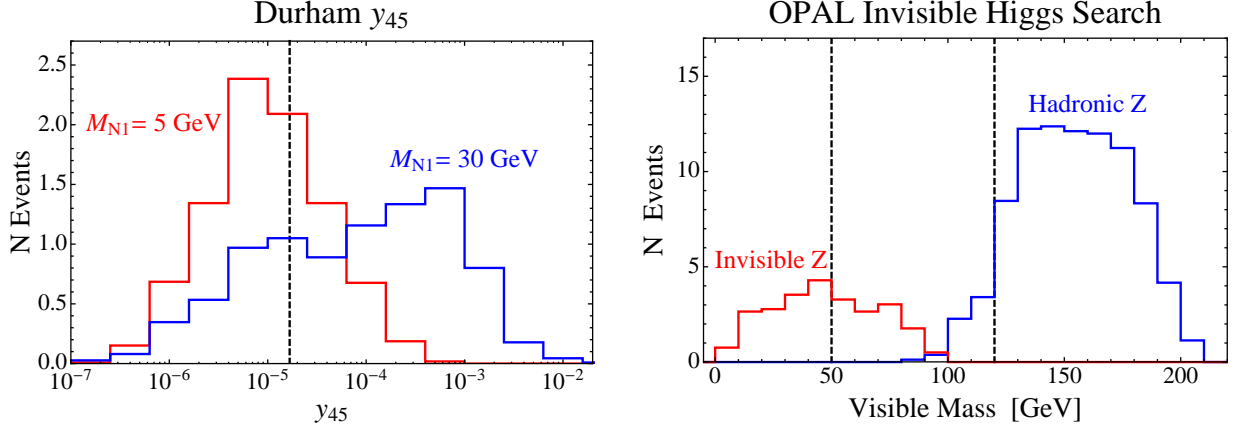


Figure 12: *Left:* The Durham y_{45} jet clustering parameter [64] for Higgs-strahlung events with leptonic Z 's. The ALEPH $h \rightarrow WW^*$ search [52], class **2c**, cuts on $y_{45} > 2 \times 10^{-5}$, selecting events with 5 well-separated objects (y_{45} is small, if the event has less than 5 well-separated jets). Due to the leptonic Z , this search is less sensitive to models where the Higgs decays to two or less lepton jets. *Right:* The visible mass distribution for Higgs-strahlung events with hadronic or invisible Z 's in the neutralino benchmark of Section 7.3. The OPAL $h \rightarrow \cancel{E}_T$ search [36] selects events with $50 \text{ GeV} < M_{\text{vis}} < 120 \text{ GeV}$. Some, but not too much, missing energy per Higgs decay, $E_T \sim 50 \text{ GeV}$, helps evade this search by keeping most invisible Z events below the window and hadronic (or leptonic) Z events above the window.

algorithm to select events with at least 5 well separated jet-like or single track objects. This subclass is sensitive to our signal from $e^+e^- \rightarrow Zh$ production, if the Z decays leptonically (forming two well-separated objects), while h decays to three or more lepton jets. Higgs production is therefore safe if the Higgs decays to less than three lepton jets, as shown on the left panel of Figure 12. We see that final states with two lepton jets are favored by both LEP-1 and LEP-2.

We note, however, that the two-lepton jet topology is partially constrained by LEP-2. In particular, searches for squark pair production target topologies with two QCD jets and missing energy, and these searches can be sensitive to Higgs decays to lepton jets accompanied by an invisible Z . We find that the OPAL squark search, [56], is most constraining, although because of the substantial SM background it does not have the sensitivity to exclude a 100 GeV Higgs decaying to lepton jets. An exception is the sneutrino channel, which is particularly constrained by [56], because of the extra lepton jet events due to direct sneutrino

production through off-shell Z 's. The ALEPH squark search, [57], is less sensitive to all channels due to tighter cuts that largely reduce the signal. LEP-2 has also searched for Higgs decays to two QCD jets. These searches do not seriously constrain Higgs decays to lepton jets because they require heavy flavor tagging and/or focus on Higgs decays without missing energy [51].

The lepton multiplicity within lepton jets is also strongly constrained by LEP-1 and LEP-2. In particular, the neutralino cannot have a large branching fraction to invisible matter. Indeed, at LEP-1, the monojet topology must be suppressed by $\sim 10^{-6}$, and therefore the neutralino branching fraction to purely missing energy, by $\sim 10^{-3}$. The ALEPH search for $h \rightarrow 4\tau$ [12] at LEP-2 constrains the multiplicity further since the search is evaded by lepton jets containing more than 4 leptons. Meanwhile, the flavor of leptons within lepton jets is most constrained at the Tevatron, where the D0 search for $h \rightarrow 4\mu, 2\mu 2\tau$ [60] sets stringent limits on final states containing muons with companion tracks. Models where lepton jets are electron only, $m_{\gamma_d} < 2m_\mu$, are unconstrained by this search. When $m_{\gamma_d} > 2m_\mu$, lepton jets consisting of exactly two muons must be suppressed by $\sim 10^{-3}$, while lepton jets with more than two leptons can spoil the track and calorimeter isolation requirements placed on the muon pairs [60]. We therefore find that high multiplicity lepton jets are the least constrained, and are necessary for models where lepton jets include muons.

The amount of missing energy per Higgs decay is most constrained by the OPAL search for $h \rightarrow \cancel{E}_T$ which selects events with a visible mass in a wide window around the Z mass, $50 \text{ GeV} < M_{\text{vis}} < 120 \text{ GeV}$. Our signal can fall within this window when Higgs decays include too much missing energy. For a light Higgs, $m_Z \sim m_h$, this search is also sensitive to the situation where the Z decays invisibly and the Higgs decays to lepton jets. Then, some missing energy can lead to a signal with $M_{\text{vis}} < 50 \text{ GeV}$, evading the search. We therefore find that hadronic and invisible Z decays constrain the missing energy from opposite directions, and the optimal value is $E_T \sim 50 \text{ GeV}$, as in the right panel of Figure 12. We also find that the sneutrino channel is more difficult to accommodate with this search than the other channels, because the sneutrino decays produce neutrinos that carry substantial missing energy. We note that a hidden Higgs decaying to final states that include missing energy is also considered by Ref. [65].

Finally, we comment that trilepton searches [44, 45] and like-sign dilepton searches [43],

are easily evaded by lepton jets due to the strong isolation requirements of these searches. Consequently, most Tevatron searches do not constrain the Higgs-to-lepton jets scenario. We summarize the consequences of existing searches at LEP and the Tevatron for a light Higgs decaying to lepton jets,

- **Two-Jet Topology:** The Higgs should decay to two lepton jets. For the neutralino channel, $m_{\tilde{N}_1} \lesssim 10$ GeV.
- **High Lepton Multiplicity:** The lepton jets should have high lepton multiplicities, $\gtrsim 4$ leptons per lepton jet.
- **All Electron or Very High Multiplicity:** All-electron lepton jets, $m_{\gamma_d} < 2 m_\mu$, are the least constrained. Very high multiplicity lepton jets can include muons, if the rate of events with isolated muon pairs, is suppressed by $\sim 10^{-3}$.
- **Some \cancel{E}_T :** The Higgs decays should produce some, but not too much, missing energy, $\cancel{E}_T \sim 50$ GeV.

7.3 Benchmarks Models

We now present one benchmark model with a 100 GeV Higgs for each of the decay channels: the neutralino channel (Section 3.1), the sneutrino channel (Section 3.2), and the singlet channel (Section 3.3). For the neutralino and sneutrino benchmarks the hidden photon decays only to electrons, whereas for the singlet benchmark muons are also produced. The neutralino and singlet benchmarks pass all searches of sections 6.1, 6.2, and 6.3 at the 2σ level, hiding the Higgs from LEP and the Tevatron. Efficiencies of the searches for each of the benchmarks are given in Appendix B. For the sneutrino model, we find some tension at accommodating all searches, when using the simple $U(1)_d$ hidden sector of Section 2.2. We present a benchmark model which is excluded by the ALEPH $h \rightarrow 4\tau$ search [12] and the OPAL $2j + \cancel{E}_T$ squark search [56] at more than 3σ , but passes all the other searches within 2σ . The tension is due to the extra lepton jet events following from $e^+e^- \rightarrow Z^* \rightarrow \tilde{\nu}\tilde{\nu}$, the missing energy carried by the neutrinos produced in the sneutrino decays, and the difficulty at achieving a 2-jet structure with sufficient lepton multiplicity. It is to be stressed that this

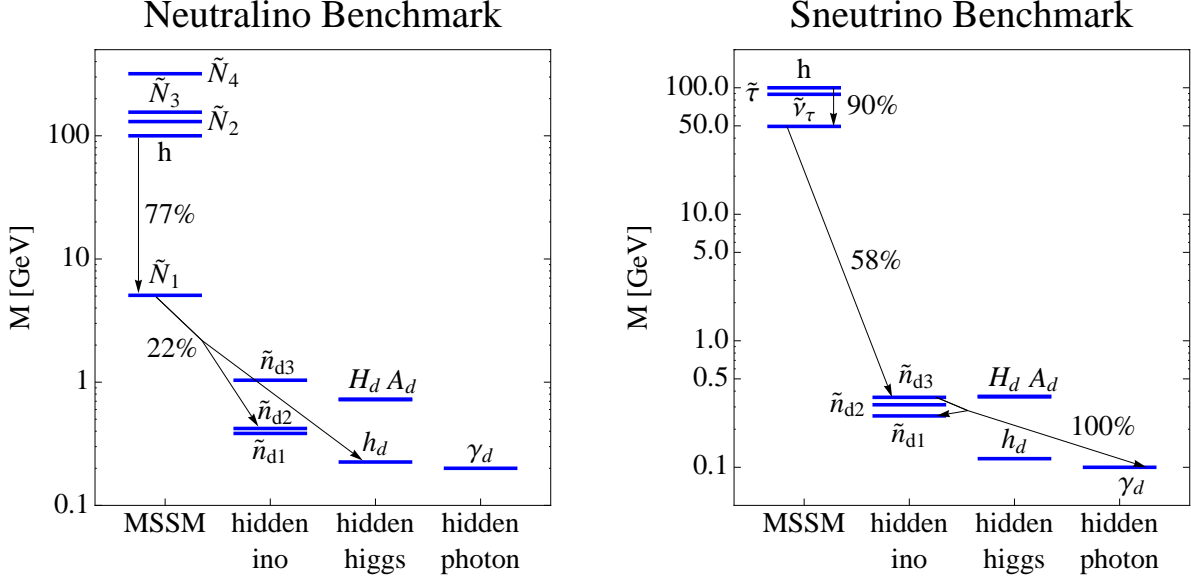


Figure 13: Spectra in the neutralino and sneutrino benchmark models. The dominant decay chain of the Higgs is denoted by arrows, labeled with branching ratios. Only the lowest lying states in the MSSM are shown. We also do not show the final decays into visible states in the last step of the decay chain. For the neutralino benchmark one has: $\tilde{n}_{d2} \rightarrow \tilde{n}_{d1} e^+ e^-$, $h_d \rightarrow \gamma_d e^+ e^-$ where in both benchmarks $\gamma_d \rightarrow e^+ e^-$ and \tilde{n}_{d1} is stable.

latter difficulty is an artifact of the particular hidden sector model we are considering, and can be ameliorated in models with longer hidden sector cascades or substantial showering.

The three benchmark models occur within the supersymmetric framework. The constraints on these models are, in principle, sensitive to all soft parameters because SUSY partners may be produced at LEP and the Tevatron, and decay to lepton jets. For this discussion, because we are interested specifically in the constraints on Higgs decays to lepton jets, we decouple all unrelated SUSY partners and only consider light soft parameters that play a role in Higgs decays. For the neutralino channel, we specify the -ino spectrum, for the sneutrino channel we specify the left-handed slepton spectrum, and for the singlet channel we specify the parameters that determine the singlet VEV and F -term. It would be interesting to relax this assumption, and study the constraints on a light Higgs accompanied by additional light SUSY partners decaying to lepton jets, and we leave this for future study.

Neutralino Benchmark. For the neutralino benchmark we take $m_h = 100$ GeV, while the

Singlet Benchmark

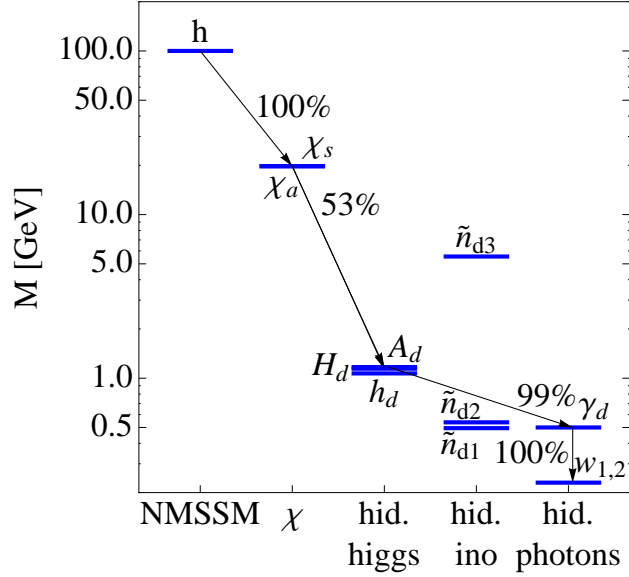


Figure 14: Spectrum of the singlet benchmark model. From the NMSSM states only the Higgs is shown, while other low lying states are also possible. The dominant decay chain of the Higgs is denoted by arrows, labeled with branching ratios. At the end of the decay chain $w_{\text{hid}}^{1,2}$ decay to e^+e^- . The LSP is \tilde{n}_{d1} .

relevant electroweak MSSM parameters are

$$\mu = 149 \text{ GeV}, \quad M_1 = 13 \text{ GeV}, \quad M_2 = 286 \text{ GeV}, \quad \tan \beta = 3.5, \quad \sin \alpha = -0.28, \quad (7.1)$$

and the hidden sector parameters are,

$$m_{\gamma_d} = 0.2 \text{ GeV}, \quad \mu_d = 0.4 \text{ GeV}, \quad M_d = 1 \text{ GeV}, \quad \tan \beta_d = 4, \quad \sin \alpha_d = -0.27, \quad (7.2)$$

where the hidden sector parameterization is defined in Appendix A. The resulting spectrum is shown in the left panel of Figure 13. Since $m_{\gamma_d} < 2m_\mu$ the lepton jets are composed entirely of electrons. Note that $m_{\tilde{N}_1} = 5 \text{ GeV}$, so that the Higgs decays produce boosted neutralinos. The resulting topology consists of 2 neutralino jets, avoiding the searches at LEP-1 and LEP-2. The lightest chargino has a mass of $m_{\tilde{C}_1} = 123 \text{ GeV}$, while the second lightest neutralino has a mass of $m_{\tilde{N}_2} = 130 \text{ GeV}$. These masses are above the LEP-2 reach. Also the Tevatron trilepton constraints do not apply because \tilde{N}_2 dominantly decays to \tilde{N}_1 and an on-shell Z . Trilepton searches veto events where opposite sign leptons reconstruct

an on-shell Z , in order to control the electroweak background [44, 45]. For this benchmark, the Z decays to neutralinos with branching fraction $\Gamma_{Z \rightarrow 2\tilde{N}_1} = 8 \times 10^{-4}$, which is consistent with the LEP-1 measurement of the Z width [50].

Sneutrino Benchmark. For the sneutrino benchmark, we also take $m_h \sim 100$ GeV. Here the Higgs decays into a pair of light tau sneutrinos. The relevant MSSM parameters are given by,

$$m_{L_3} = 77.3 \text{ GeV}, \quad \tan \beta = 3.5, \quad \sin \alpha = -0.28, \quad (7.3)$$

and the parameters that determine the hidden sector spectrum are,

$$m_{\gamma_d} = 0.1 \text{ GeV}, \quad \mu_d = 0.3 \text{ GeV}, \quad M_d = 0.3 \text{ GeV}, \quad \tan \beta_d = 4, \quad \sin \alpha_d = -0.27. \quad (7.4)$$

The spectrum is shown in the right panel of Figure 13. The hidden photon decays only to electrons. The tau sneutrino has a mass of $m_{\tilde{\nu}_\tau} = 49.5$ GeV and the stau a mass of $m_{\tilde{\tau}} = 89$ GeV. The stau and tau sneutrino are pair produced at LEP through an off-shell Z , leading to a lepton jet signal. For reference, the LEP-2 cross-sections of Higgs-strahlung, tau sneutrino pair production, and stau pair production are, at $\sqrt{s} = 206$ GeV, $\sigma_{hZ} \simeq 0.3$ pb, $\sigma_{\tilde{\nu}\tilde{\nu}} \simeq 0.3$ pb, and $\sigma_{\tilde{\tau}\tilde{\tau}} \simeq 0.1$ pb. We find that this benchmark is ruled out by the ALEPH $h \rightarrow 4\tau$ search [12] and the OPAL $2j + \cancel{E}_T$ squark search [56], both at more than 3σ , while it passes all other searches at or below 2σ . The ALEPH search is only sensitive to lepton jets with low multiplicity and can be evaded by models that produce extra leptons through longer cascades or sufficient hidden sector showering.

Singlet Benchmark. The singlet benchmark also has a SM like Higgs at 100 GeV. In this model, the NMSSM singlet S couples to hidden sector messengers χ and $\bar{\chi}$, which couple to the hidden sector Higgses $h_{1,2}$ (see equation 3.8). The relevant NMSSM parameters [66] are given by,

$$\begin{aligned} \langle S \rangle = 150 \text{ GeV}, \quad \lambda = 1, \quad \kappa = 2, \quad \tan \beta = 5, \\ A_\lambda = 10, \quad A_\kappa = 1, \end{aligned} \quad (7.5)$$

and the hidden sector parameters are given by,

$$\begin{aligned} m_\chi = 160 \text{ GeV}, \quad \mu_d = 0.5 \text{ GeV}, \quad m_{\gamma_d} = 0.5 \text{ GeV}, \quad \tan \beta_d = 2, \\ M_d = 5.5 \text{ GeV}, \quad B\mu_d = -0.5, \text{ GeV}^2, \quad \kappa_1 = 0.1, \quad \kappa_2 = 0.1. \end{aligned} \quad (7.6)$$

Here, m_χ denotes the mass of the fermionic messengers, which are proportional to $\langle S \rangle$. The spectrum is shown in Figure 14. The scalar messengers, χ_\pm , are split by $\langle F_S \rangle$. The lighter scalar messenger has a mass of 20 GeV, allowing for the Higgs decays, $h \rightarrow \chi_- \chi_-^*$. For this benchmark, we include muon production, which as discussed above, requires substantial lepton multiplicity in order to evade the D0 search for $h \rightarrow 4\mu, 2\mu 2\tau$ [60]. We find this difficult to achieve with the simplest $U(1)_d$ hidden sector, so for this benchmark we extend the hidden sector to a larger non-Abelian group, $SU(2)_d \supset U(1)_d$, where we take hidden sector cascades to dominantly end with decays of the form $\gamma_d \rightarrow w_d^1 w_d^2 \rightarrow 2 l^- l^+$.

8 Suggested Search Strategies

We have argued that signatures of the Higgs decaying into lepton jets could have gone unnoticed by existing collider searches, especially if the leptons are collimated into two jets, mimicking the topology of certain hadronic backgrounds. Nevertheless, several properties of the lepton jets set them apart from QCD jets, and dedicated searches could very likely extract the signal from the SM background. Below we point out some features of the signal that could be targeted by experiments in order to increase the sensitivity. The discussion is concise and qualitative; a more quantitative study is beyond the scope of this paper and will be attempted elsewhere [67].

- **Hadronic energy deposition.** An obvious consequence of the high lepton content of the jets is a small energy fraction deposited in the hadronic calorimeter. Typical electrons stop in the electromagnetic calorimeter, while typical muons deposit of order 1-2 GeV in the hadronic calorimeter. Therefore experiments could search for jets with an anomalously small $E_{\text{had}}/E_{\text{em}}$ ratio.
- **Event shapes.** Since the leptons originate from highly boosted objects, lepton jets are slimmer than typical QCD jets. This is shown in Fig. 15 where we compare the transverse momentum as a function of the jet radius for lepton jets and QCD jets [68]. The main parameter setting the size (defined, e.g., by the cone where 90% of the jet energy resides) is the ratio of the hidden photon mass to the electroweak scale. For the parameter choices considered in this paper, typical lepton jet sizes are $\Delta R \lesssim 0.1$,

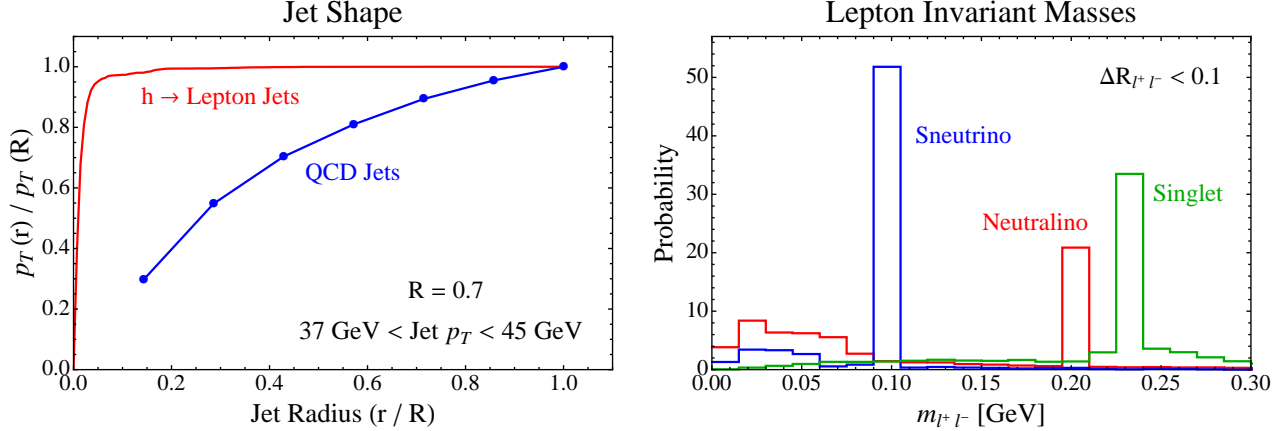


Figure 15: Lepton jet shape and constituent invariant masses. *Left:* We compare the shape of lepton jets produced by Higgs decays to the shape of QCD jets, as measured by CDF [68]. Jets of size $R = 0.7$ are identified by clustering the event with a midpoint-cone algorithm. The jet shape is then defined as the p_T fraction contained in smaller cones. We see that lepton jets are much narrower than QCD jets. *Right:* The invariant masses of all opposite sign lepton pairs, separated by $\Delta R < 0.1$, in Higgs decays to lepton jets. We see clear invariant mass peaks corresponding to the hidden sector photon masses, despite the background of wrong-pair combinatorics. Both jet shape and invariant mass peaks can be used to overcome the QCD background and discover lepton jets.

compared to $\Delta R \sim 0.7$ for QCD jets. We stress that this estimates will change if hidden sector showering is significant, $g_d^2/4\pi \gtrsim 0.1$. An experiment could therefore impose cuts on the energy or p_T in the $0.1 < \Delta R < 0.4$ cone, as proposed in [15].

- **Pair invariant mass.** Many lepton pairs in the jets originate from two-body decays of the hidden photons. Therefore the invariant mass of the pair reconstructs the hidden photon mass. One can pair opposite sign same flavor leptons separated by, say, $\Delta R = 0.1$, and compute the invariant mass of all the pairs. The signal sample displays a prominent peak at the invariant mass of the hidden photon despite the combinatoric background. The peaks are clearly visible in Fig. 15 for the three benchmark points described in Section 7.
- **Leptons in jets.** Lepton jets in our scenario are composed of electrons, and possibly muons, with high multiplicities of leptons within each jet. QCD jets also contain leptons, but many of them originate from decays of pions and kaons in-flight. Prompt or

almost prompt leptons can be produced by semileptonic decays of bottom and charm mesons, but these typically lead to 1 or 2 prompt leptons per jet. Experiments could therefore search for jets with an anomalous lepton content. Repeating the analysis of [12] without demanding the small number of tracks inside the lepton jet, but using instead the jet shape, hadronic energy or lepton ID information to control the background, could allow for sufficient sensitivity to discover a light Higgs decaying to lepton jets.

The above characteristics of lepton jets can be used to develop Tevatron searches, and to re-analyze old LEP-1 and LEP-2 data. For a 100 GeV hidden Higgs there are enough potential signal events to make such searches promising. We predict on the order of 100 Higgs events at LEP-2, and on the order of 10^4 Higgs events at the Tevatron. Furthermore, the light neutralino scenario could lead to up to 10^4 lepton jet events at LEP-1. This is substantially more than in the case where no light SUSY state is present in which case the Z branching fraction to the hidden sector is suppressed by $\epsilon^2 \lesssim 10^{-6}$ and the number of lepton jets at LEP-1 is at most $\mathcal{O}(1)$ [16]. We conclude that a huge event sample might be buried in the existing data waiting to be uncovered! The precise sensitivity of experiments crucially depends on the experimental ability to reconstruct nearby tracks, untangle overlapping calorimetric showers, and identify nearby leptons. These issues are difficult to estimate without a full and accurate detector simulation and therefore input from the experimental community is vital.

9 Conclusions and Outlook

The mass and the decay width of a SM-like Higgs are strongly constrained by LEP and Tevatron searches. In the supersymmetric framework the existing bounds imply the need for fine tuning. These bounds (and hence the fine tuning) may be ameliorated if the Higgs has non-standard decays. Similarly, existing bounds on the masses of SM superpartners may be evaded if they decay unconventionally. It is therefore conceivable that both the Higgs and (possibly some of) the superpartners are sufficiently light to have been copiously produced at LEP and the Tevatron. Searches for standard decays could have missed such hidden states.

In this paper we studied the prospects for the Higgs, and possibly the lightest neutralino

or sneutrino, to be hidden at colliders due to their dominant decays into states that are part of a low scale hidden sector weakly coupled to the SM. The hidden states then subsequently cascade decay back to electrons and muons. The low, $\mathcal{O}(\text{GeV})$, mass gap in the hidden sector together with the hidden cascade decays, imply a significant number of collimated final state leptons known as lepton jets. Here we have considered three channels where the Higgs first decays to two light neutralinos, light sneutrinos or directly to the hidden sector fields. Due to the mixing between the SM and the hidden sector, the lightest visible supersymmetric particle is no longer stable and hidden cascade decays occur. In all cases, the branching fraction of the Higgs to the hidden sector can dominate.

To test these scenarios we have identified the main experimental observables that characterize the collider signals of these models. We then simulated and studied existing SUSY and Higgs searches at LEP and the Tevatron that are potentially sensitive to lepton jets. Quite surprisingly, we found that the Higgs can evade detection if it *decays to some amount of missing energy together with many non-isolated electron or muons, all residing in two jet-like structures*. The topology and the lepton multiplicity depend on the spectrum of both the hidden and the visible sectors. Interestingly, the required phenomenology is easily produced by the minimal hidden sector model. Our study suggests that bounds on many additional SM superpartners may be significantly weakened in the presence of a low scale hidden sector. Consequently, other superpartners, not studied in this work, may be hidden at LEP or the Tevatron.

It would be very interesting to assess the potential for a discovery of this scenario in colliders [67]. One very effective path would be to reanalyze the old LEP data. A dedicated LEP-2 search for Z +lepton jets should easily extract the signal of Higgs-to-lepton jet decays from the background or significantly improve the bound on the mass of the Higgs in this scenario. Revisiting LEP-1 data may also be rewarding, because in the light neutralino scenario as many as 10^4 lepton jets (which we dub neutralino jets) could have been produced. Finally, the prospects at the Tevatron and the LHC also look promising, given the large number of final-state leptons. All experiments could increase their sensitivity to our scenario by zooming in on narrow jets with small hadronic deposits, attempting reconstruction of prompt leptons inside jets, counting their multiplicities, and studying the invariant mass distribution of close lepton pairs. So far dedicated experimental searches were limited to

finding isolated lepton pairs. Our work suggests that this approach could be too narrow, and higher multiplicities of collimated leptons should also be targeted. To do so a serious study incorporating detector simulation is therefore warranted.

Finally, we stress that the relevance of our work extends beyond this particular hidden Higgs scenario. Even if the Higgs boson is heavier than 115 GeV, Higgs and/or SM superpartners decaying to light SM states via a hidden sector is a phenomenological possibility that deserves attention. The standard new physics signatures may be altered or completely absent, and the signal would be missed unless it is specifically searched for. Multiple theoretical possibilities should be explored in order to ensure that such a scenario is not overlooked at the LHC.

Acknowledgments

We thank Nima Arkani-Hamed, Kyle Cranmer, Csaba Csaki, JiJi Fan, David Krohn, Matt Reece, Liantao Wang and Itay Yavin for useful discussions. We would especially like to thank Christophe Delaere, Yuri Gershtein, and Chris Tully for very useful discussions about LEP and the Tevatron. The work of AF was supported in part by the Department of Energy grant DE-FG02-96ER40949. JTR is supported by an NSF graduate fellowship. TV is supported by DOE grant DE-FG02-90ER40542. The work of JZ is supported in part by the European Commission RTN network, Contract No. MRTN-CT-2006-035482 (FLAVIANet) and by the Slovenian Research Agency.

A Notation

The visible sector is the ordinary MSSM, and we follow the notation of [66]. The hidden sector is a broken supersymmetric U(1) gauge theory with 2 Higgs multiplets $h_{1,2}$ of opposite U(1) charge and the superpotential $W = \mu_d h_1 h_2$ [15]. Such a theory is completely specified by 3 scalar soft mass terms $m_{1,2}^2$, $B\mu_d$, the hidden bino mass M_d , the mu-term μ_d and the gauge coupling g_d . We do not impose any constraints on these parameters, in particular we do not assume any specific mechanism of supersymmetry breaking mediation to the dark

sector. The scalar potential takes the form

$$V = (m_1^2 + \mu_d^2)|h_1|^2 + (m_2^2 + \mu_d^2)|h_2|^2 + (B\mu_d h_1 h_2 + \text{h.c.}) + \frac{g_d^2}{2} (|h_1|^2 - |h_2|^2)^2. \quad (\text{A.1})$$

We are interested in the regions of the parameter space where the hidden scalars acquire vevs, $\langle h_1 \rangle = \sin \beta_d v_d$, $\langle h_2 \rangle = \cos \beta_d v_d$, which gives the hidden photon the mass $m_{\gamma D} = g_d v_d$. In the broken phase, it is convenient to trade the scalar soft mass terms for more physical parameters: v_d , β_d and the mixing angle α_d of the two CP-even mass eigenstates h_d, H_d . The physical scalars are embedded in the Higgs fields as

$$\begin{aligned} h_1 &= \frac{\sin \beta_d v_d + \cos \alpha_d h_d + \sin \alpha_d H_d + i \cos \beta_d A_d}{\sqrt{2}} \\ h_2 &= \frac{\cos \beta_d v_d - \sin \alpha_d h_d + \cos \alpha_d H_d + i \sin \beta_d A_d}{\sqrt{2}} \end{aligned} \quad (\text{A.2})$$

where A_d is the CP-odd scalar eigenstate. At the tree level the mass of the lighter Higgs h_d is constrained to be $\leq m_{\gamma D}$, in analogy with the MSSM. However loop corrections from the hidden gauge and Higgs multiplets or from additional multiplets in the hidden sector can change that relation. Additional couplings to heavier hidden states can also contribute to the hidden Higgs mass. Therefore we take m_{h_d} as a free parameter of order $m_{\gamma D}$ when constructing our benchmark models. In the fermionic sector the mass terms after U(1) breaking are

$$- m_{\gamma D} \sin \beta_d \tilde{h}_1 \tilde{b} + m_{\gamma D} \cos \beta_d \tilde{h}_2 \tilde{b} - \frac{M_d}{2} \tilde{b} \tilde{b} - \mu_d \tilde{h}_1 \tilde{h}_2 + \text{h.c.} \quad (\text{A.3})$$

The physical fermions are 3 dark neutralinos who are mixtures of hidden binos and higgsinos.

B Efficiencies of the Searches

In this appendix we quote the efficiencies of selected experimental analyses to the signals from the 3 benchmark models of Section 3. In Table 1 we list the number of the observed events in each of the searches after all the cuts are applied (Obs.), the expected number of SM background events (Bckg.), and the predicted number of signal events for the three benchmarks: the neutralino channel (Neutr.), the sneutrino channel (Sneutr.) and the singlet channel (Singlet). This should be compared to the maximum number of signal events (Max.)

LEP-1 searches							
Search	Ref.	Obs.	Bckg.	Neutr.	Sneutr.	Singlet	Max.
Monojets	[42]	3	2.8	< 1	0	0	6.6
Acoplanar	[41]	0	0.2	< 1	0	0	3.8
LEP-2 searches							
Search	Ref.	Obs.	Bckg.	Neutr.	Sneutr.	Singlet	Max.
$H \rightarrow 4\tau$	[12]	2	5.09	1	15	1	5.0
$H \rightarrow \cancel{E}$	[36]	8	11	2	5	3	7.5
$H \rightarrow WW^*2c$	[52]	0	0.3	2	< 1	2	3.8
$H \rightarrow WW^*2t$	[52]	1	1.2	1	1	3	5.0
6l	[55]	1	1.1	< 1	4	< 1	5.0
$2j + \cancel{E}$ (OPAL)	[56]	13	19.8	8	35	7	7.8
$2j + \cancel{E}$ (ALEPH)	[57]	19	15.9	7	3	1	14.5
$2j + 2l + \cancel{E}$	[57]	5	3	2	4	5	9.0
Tevatron searches							
Search	Ref.	Obs.	Bckg.	Neutr.	Sneutr.	Singlet	Max.
Dark photon	[59]	7	8	~ 1	< 1	< 1	7.9
$H \rightarrow 4\mu$	[60]	2	2.2	0	0	2	5.8
Unified 3l	[44]	1	1.47	< 1	< 1	< 1	3.7
Low p_T 3l	[45]	1	0.4	< 1	< 1	< 1	5.4
Like-sign 2l	[43]	13	7.8	1	< 1	< 1	14.7

Table 1: A compilation of relevant searches for constraining the Higgs-to-lepton jet events.

allowed at the 97.7% confidence level. This corresponds to a $2\text{-}\sigma$ one sided "exclusion" for Gaussian errors. The confidence level is determined using the CL_s prescription used at LEP for Higgs searches and takes into account downward fluctuations in the data compared to the expected background [69, 70]. The searches that do not pass the 2-sigma threshold are denoted in bold.

The numbers of observed events and the background estimates given in Table 1 refer to

the following:

- $H \rightarrow 4\tau$ search: invisible Z channel, $n_{1,2}^{\text{track}} = 2$ or 4, see Table 3 of [12],
- Invisible Higgs search in OPAL: more-than-2-jet events with M_{miss} in the 100-104 GeV bin, see Fig.4 in [36],
- $H \rightarrow WW^*$ search in ALEPH: the class 2c and 2t defined in Table 3 of [52],
- Six-lepton search in ALEPH: small Δm selection defined in Table 3.4 of [55],
- $2j + \cancel{E}$ search in OPAL and ALEPH: selection A, see Table 2 of [56], and large Δm AJ selection (years 1999-2000), see Table 5 of [57],
- $2j + 2l + \cancel{E}$ in ALEPH: to the large Δm selection (years 1999-2000), see Table 5 of [57]
- Dark photon search in D0: electron pairs with 0.2-0.4 GeV invariant mass, see Fig. 2 of [59],
- Unified trilepton search in CDF: trileptons defined by the (least tight) ttt cut, see Table 1 of [44],
- Like-sign dilepton search in CDF: dilepton events with missing energy, see Table 2 of [43].

The signal predictions were obtained using monte carlo as explained in Section 7.1.

References

- [1] R. Barate *et al.* Phys. Lett. B **565**, 61 (2003) [arXiv:hep-ex/0306033].
- [2] H. Flacher, M. Goebel, J. Haller, A. Hocker, K. Moenig and J. Stelzer, Eur. Phys. J. C **60**, 543 (2009) [arXiv:0811.0009 [hep-ph]].
- [3] R. E. Shrock and M. Suzuki, Phys. Lett. B **110**, 250 (1982). B. A. Dobrescu and K. T. Matchev, JHEP **0009**, 031 (2000) [arXiv:hep-ph/0008192]; D. O’Connell,

- M. J. Ramsey-Musolf and M. B. Wise, Phys. Rev. D **75**, 037701 (2007) [arXiv:hep-ph/0611014]. O. Bahat-Treidel, Y. Grossman and Y. Rozen, JHEP **0705**, 022 (2007) [arXiv:hep-ph/0611162]; K. Cheung, J. Song and Q. S. Yan, Phys. Rev. Lett. **99**, 031801 (2007) [arXiv:hep-ph/0703149].
- [4] S. Schael *et al.* Eur. Phys. J. C **47**, 547 (2006) [arXiv:hep-ex/0602042].
- [5] S. Chang, R. Dermisek, J. F. Gunion and N. Weiner, Ann. Rev. Nucl. Part. Sci. **58**, 75 (2008) [arXiv:0801.4554 [hep-ph]].
- [6] R. Dermisek, Mod. Phys. Lett. A **24**, 1631 (2009) [arXiv:0907.0297 [hep-ph]].
- [7] R. Dermisek and J. F. Gunion, Phys. Rev. Lett. **95**, 041801 (2005) [arXiv:hep-ph/0502105]; R. Dermisek and J. F. Gunion, Phys. Rev. D **75**, 075019 (2007) [arXiv:hep-ph/0611142]. R. Dermisek and J. F. Gunion, arXiv:1002.1971 [hep-ph].
- [8] S. Chang, P. J. Fox and N. Weiner, JHEP **0608**, 068 (2006) [arXiv:hep-ph/0511250].
- [9] B. Bellazzini, C. Csaki, A. Falkowski and A. Weiler, Phys. Rev. D **80**, 075008 (2009) [arXiv:0906.3026 [hep-ph]]; B. Bellazzini, C. Csaki, A. Falkowski and A. Weiler, arXiv:0910.3210 [hep-ph].
- [10] L. M. Carpenter, D. E. Kaplan and E. J. Rhee, Phys. Rev. Lett. **99**, 211801 (2007) [arXiv:hep-ph/0607204].
- [11] M. S. Carena, J. R. Ellis, A. Pilaftsis and C. E. M. Wagner, Nucl. Phys. B **586**, 92 (2000) [arXiv:hep-ph/0003180]. M. S. Carena, J. R. Ellis, S. Mrenna, A. Pilaftsis and C. E. M. Wagner, Nucl. Phys. B **659**, 145 (2003) [arXiv:hep-ph/0211467].
- [12] ALEPH Collaboration, arXiv:1003.0705 [hep-ex].
- [13] G. Abbiendi *et al.* [OPAL Collaboration], Eur. Phys. J. C **27**, 311 (2003) [arXiv:hep-ex/0206022].
- [14] N. Arkani-Hamed and N. Weiner, JHEP **0812**, 104 (2008) [arXiv:0810.0714 [hep-ph]].
- [15] C. Cheung, J. T. Ruderman, L. T. Wang and I. Yavin, arXiv:0909.0290 [hep-ph].

- [16] M. Baumgart, C. Cheung, J. T. Ruderman, L. T. Wang and I. Yavin, JHEP **0904**, 014 (2009) [arXiv:0901.0283 [hep-ph]].
- [17] M. J. Strassler and K. M. Zurek, Phys. Lett. B **651**, 374 (2007) [arXiv:hep-ph/0604261].
T. Han, Z. Si, K. M. Zurek and M. J. Strassler, JHEP **0807**, 008 (2008) [arXiv:0712.2041 [hep-ph]].
M. J. Strassler, arXiv:hep-ph/0607160.
- [18] O. Adriani *et al.* [PAMELA Collaboration], Nature **458**, 607 (2009) [arXiv:0810.4995 [astro-ph]].
- [19] F. Aharonian *et al.* [H.E.S.S. Collaboration], Phys. Rev. Lett. **101**, 261104 (2008) [arXiv:0811.3894 [astro-ph]]; Astron. Astrophys. **508**, 561 (2009) [arXiv:0905.0105 [astro-ph.HE]].
- [20] A. A. Abdo *et al.* [Fermi LAT Collaboration], Phys. Rev. Lett. **102**, 181101 (2009) [arXiv:0905.0025 [astro-ph.HE]].
- [21] N. Arkani-Hamed, D. P. Finkbeiner, T. R. Slatyer and N. Weiner, Phys. Rev. D **79**, 015014 (2009) [arXiv:0810.0713 [hep-ph]].
- [22] P. Meade, M. Papucci, A. Strumia and T. Volansky, arXiv:0905.0480 [hep-ph].
- [23] M. Pospelov and A. Ritz, Phys. Lett. B **671**, 391 (2009) [arXiv:0810.1502 [hep-ph]].
- [24] I. Z. Rothstein, T. Schwetz and J. Zupan, JCAP **0907**, 018 (2009) [arXiv:0903.3116 [astro-ph.HE]].
- [25] C. Cheung, J. T. Ruderman, L. T. Wang and I. Yavin, Phys. Rev. D **80**, 035008 (2009) [arXiv:0902.3246 [hep-ph]]; A. Katz and R. Sundrum, JHEP **0906**, 003 (2009) [arXiv:0902.3271 [hep-ph]].
- [26] E. J. Chun and J. C. Park, JCAP **0902** (2009) 026 [arXiv:0812.0308 [hep-ph]].
- [27] J. T. Ruderman and T. Volansky, arXiv:0908.1570 [hep-ph]; X. Chen, JCAP **0909** (2009) 029 [arXiv:0902.0008 [hep-ph]]; J. Mardon, Y. Nomura and J. Thaler, Phys. Rev. D **80** (2009) 035013 [arXiv:0905.3749 [hep-ph]].

- [28] M. J. Strassler and K. M. Zurek, Phys. Lett. B **661** (2008) 263 [arXiv:hep-ph/0605193].
- [29] S. Gopalakrishna, S. Jung and J. D. Wells, Phys. Rev. D **78**, 055002 (2008) [arXiv:0801.3456 [hep-ph]].
- [30] B. Batell, M. Pospelov and A. Ritz, Phys. Rev. D **80** (2009) 095024 [arXiv:0906.5614 [hep-ph]].
- [31] B. Holdom, Phys. Lett. B **166** (1986) 196.
- [32] M. Pospelov, A. Ritz and M. B. Voloshin, Phys. Lett. B **662** (2008) 53 [arXiv:0711.4866 [hep-ph]].
- [33] B. Batell, M. Pospelov and A. Ritz, Phys. Rev. D **79** (2009) 115008 [arXiv:0903.0363 [hep-ph]].
- [34] M. Ahlers, J. Jaeckel, J. Redondo and A. Ringwald, Phys. Rev. D **78**, 075005 (2008) [arXiv:0807.4143 [hep-ph]]; Y. Bai and Z. Han, Phys. Rev. Lett. **103**, 051801 (2009) [arXiv:0902.0006 [hep-ph]]; R. Essig, P. Schuster and N. Toro, Phys. Rev. D **80** (2009) 015003 [arXiv:0903.3941 [hep-ph]]; M. Reece and L. T. Wang, JHEP **0907** (2009) 051 [arXiv:0904.1743 [hep-ph]]; J. D. Bjorken, R. Essig, P. Schuster and N. Toro, Phys. Rev. D **80** (2009) 075018 [arXiv:0906.0580 [hep-ph]]; M. Goodsell, J. Jaeckel, J. Redondo and A. Ringwald, JHEP **0911**, 027 (2009) [arXiv:0909.0515 [hep-ph]]; M. Freytsis, G. Ovanessian and J. Thaler, arXiv:0909.2862 [hep-ph]; P. Schuster, N. Toro and I. Yavin, Phys. Rev. D **81** (2010) 016002 [arXiv:0910.1602 [hep-ph]]; P. Meade, S. Nussinov, M. Papucci and T. Volansky, arXiv:0910.4160 [hep-ph]; R. Essig, P. Schuster, N. Toro and B. Wojtsekhowski, arXiv:1001.2557 [hep-ph].
- [35] D. E. Morrissey, D. Poland and K. M. Zurek, JHEP **0907**, 050 (2009) [arXiv:0904.2567 [hep-ph]].
- [36] G. Abbiendi *et al.* [OPAL Collaboration], arXiv:0707.0373 [hep-ex].
- [37] J. D. Mason, D. E. Morrissey and D. Poland, Phys. Rev. D **80** (2009) 115015 [arXiv:0909.3523 [hep-ph]].

- [38] A. Djouadi, J. Kalinowski and M. Spira, *Comput. Phys. Commun.* **108**, 56 (1998) [arXiv:hep-ph/9704448].
- [39] P. Meade, M. Papucci and T. Volansky, *JHEP* **0912** (2009) 052 [arXiv:0901.2925 [hep-ph]].
- [40] C. Amsler *et al.* [Particle Data Group], *Phys. Lett. B* **667**, 1 (2008).
- [41] D. Buskulic *et al.* [ALEPH Collaboration], *Phys. Lett. B* **313**, 299 (1993).
- [42] D. Buskulic *et al.* [ALEPH Collaboration], *Phys. Lett. B* **334**, 244 (1994).
- [43] A. Abulencia *et al.* [CDF Collaboration], *Phys. Rev. Lett.* **98**, 221803 (2007) [arXiv:hep-ex/0702051].
- [44] The CDF Collaboration, CDF Public Note 9817 (2009), "*Update of the Unified Trilepton Search with 3.2 fb⁻¹ of Data*", available on www-cdf.fnal.gov/physics/exotic/r2a/20090521.trilepton_3fb
- [45] T. Aaltonen *et al.* [CDF Collaboration], *Phys. Rev. D* **79**, 052004 (2009) [arXiv:0810.3522 [hep-ex]].
- [46] M. L. Graesser, *Phys. Rev. D* **76**, 075006 (2007) [arXiv:0704.0438 [hep-ph]]; M. L. Graesser, arXiv:0705.2190 [hep-ph].
- [47] G. Choudalakis, et al., [CDF Collaboration], CDF note 8763, available at www-cdf.fnal.gov/physics/exotic/r2a/20070426.vista_sleuth/publicPage.html
- [48] R. Barate *et al.* [LEP Working Group for Higgs boson searches], *Phys. Lett. B* **565**, 61 (2003) [arXiv:hep-ex/0306033].
- [49] [LEP Higgs Working Group for Higgs boson searches], arXiv:hep-ex/0107032.
- [50] [LEP], *Phys. Rept.* **427**, 257 (2006) [arXiv:hep-ex/0509008].
- [51] G. Abbiendi *et al.* [OPAL Collaboration], *Phys. Lett. B* **597**, 11 (2004) [arXiv:hep-ex/0312042].

- [52] S. Schael *et al.* [ALEPH Collaboration], Eur. Phys. J. C **49**, 439 (2007) [arXiv:hep-ex/0605079].
- [53] A. Heister *et al.* [ALEPH Collaboration], Eur. Phys. J. C **25**, 1 (2002) [arXiv:hep-ex/0201013].
- [54] J. Abdallah *et al.* [DELPHI Collaboration], Eur. Phys. J. C **36**, 1 (2004) [Eur. Phys. J. C **37**, 129 (2004)] [arXiv:hep-ex/0406009].
- [55] A. Garcia-Bellido, arXiv:hep-ex/0212024.
- [56] G. Abbiendi *et al.* [OPAL Collaboration], Phys. Lett. B **545** (2002) 272 [Erratum-ibid. B **548** (2002) 258] [arXiv:hep-ex/0209026].
- [57] A. Heister *et al.* [ALEPH Collaboration], Phys. Lett. B **537** (2002) 5 [arXiv:hep-ex/0204036].
- [58] T. Aaltonen *et al.* [CDF Collaboration], arXiv:0810.5357 [hep-ex].
- [59] V. M. Abazov *et al.* [D0 Collaboration], Phys. Rev. Lett. **103**, 081802 (2009) [arXiv:0905.1478 [hep-ex]].
- [60] V. M. Abazov *et al.* [D0 Collaboration], Phys. Rev. Lett. **103**, 061801 (2009) [arXiv:0905.3381 [hep-ex]].
- [61] J. Alwall *et al.*, JHEP **0709**, 028 (2007) [arXiv:0706.2334 [hep-ph]].
- [62] P. Meade and M. Reece, arXiv:hep-ph/0703031.
- [63] `SlowJet` is a private `Mathematica` package for event analysis, to be distributed upon demand.
- [64] S. Moretti, L. Lonnblad and T. Sjostrand, JHEP **9808**, 001 (1998) [arXiv:hep-ph/9804296].
- [65] S. Chang and N. Weiner, JHEP **0805**, 074 (2008) [arXiv:0710.4591 [hep-ph]].
- [66] S. P. Martin, arXiv:hep-ph/9709356.

- [67] A. Falkowski, J. Ruderman, T. Volansky, J. Zupan, *in preparation*.
- [68] D. E. Acosta *et al.* [CDF Collaboration], Phys. Rev. D **71** (2005) 112002 [arXiv:hep-ex/0505013].
- [69] A.L. Read, *Modified frequentist analysis of search results (the CLs method)*, in F. James, L. Lyons, and Y. Perrin (eds.), Workshop on Confidence Limits, CERN Yellow Report 2000-005, available on cdsweb.cern.ch.
- [70] T. Junk, Nucl. Instrum. Meth. A **434**, 435 (1999) [arXiv:hep-ex/9902006].